XRCC1: a potential prognostic and immunological biomarker in LGG based on systematic pan-cancer analysis

Guobing Wang[1,2,*], Yunyue Li[3,*], Rui Pan[4,*], Xisheng Yin[4], Congchao Jia[4], Yuchen She[4], Luling Huang[5], Guanhu Yang[6], Hao Chi[4], Gang Tian[1]

[1]Department of Laboratory Medicine, The Affiliated Hospital of Southwest Medical University, Luzhou, China
[2]Medical Clinical Laboratory, Yibin Hospital of T.C.M, Yibin, China
[3]Queen Mary College, Medical School of Nanchang University, Nanchang, China
[4]Clinical Medical College, Southwest Medical University, Luzhou, China
[5]Department of Dermatology, Xijing Hospital, Fourth Military Medical University, Xi'an, China
[6]Department of Specialty Medicine, Ohio University, Athens, OH 45701, USA
*Equal contribution and share first authorship

Correspondence to: Guanhu Yang, Hao Chi, Gang Tian; email: guanhuyang@gmail.com, https://orcid.org/0000-0001-7888-5759; Chihao7511@163.com, https://orcid.org/0000-0002-5210-0770; tiangang@swmu.edu.cn
Keywords: X-ray repair cross-complementation group 1, pan-cancer, prognosis, immune infiltration, tumor microenvironment
Received: June 26, 2023   Accepted: December 1, 2023   Published: January 12, 2023

ABSTRACT

X-ray repair cross-complementation group 1 (XRCC1) is a pivotal contributor to base excision repair, and its dysregulation has been implicated in the oncogenicity of various human malignancies. However, a comprehensive pan-cancer analysis investigating the prognostic value, immunological functions, and epigenetic associations of XRCC1 remains lacking. To address this knowledge gap, we conducted a systematic investigation employing bioinformatics techniques across 33 cancer types. Our analysis encompassed XRCC1 expression levels, prognostic and diagnostic implications, epigenetic profiles, immune and molecular subtypes, Tumor Mutation Burden (TMB), Microsatellite Instability (MSI), immune checkpoints, and immune infiltration, leveraging data from TCGA, GTEx, CELL, Human Protein Atlas, Ualcan, and cBioPortal databases. Notably, XRCC1 displayed both positive and negative correlations with prognosis across different tumors. Epigenetic analysis revealed associations between XRCC1 expression and DNA methylation patterns in 10 cancer types, as well as enhanced phosphorylation. Furthermore, XRCC1 expression demonstrated associations with TMB and MSI in the majority of tumors. Interestingly, XRCC1 gene expression exhibited a negative correlation with immune cell infiltration levels, except for a positive correlation with M1 and M2 macrophages and monocytes in most cancers. Additionally, we observed significant correlations between XRCC1 and immune checkpoint gene expression levels. Lastly, our findings implicated XRCC1 in DNA replication and repair processes, shedding light on the precise mechanisms underlying its oncogenic effects. Overall, our study highlights the potential of XRCC1 as a prognostic and immunological pan-cancer biomarker, thereby offering a novel target for tumor immunotherapy.

INTRODUCTION

Cancer represents a significant global public health challenge and is poised to surpass cardiovascular disease as the primary cause of non-natural mortality in many countries, based on prevailing year-to-year trends [1–8]. Recent reports indicate that in the year 2023, the United States is projected to witness 1,958,310 new

cancer cases, with an estimated 609,820 cancer-related deaths [9]. Among the diverse spectrum of cancer types, low-grade gliomas (LGGs), classified as WHO grade II gliomas, represent a prevalent form of primary intracranial tumors, accounting for approximately 15-25% of all gliomas [10]. The annual incidence of LGGs is estimated to be around 1 case per 10,000 individuals. Notably, these tumors exhibit diffuse infiltration, gradual growth, and substantial genetic and transcriptional heterogeneity [11, 12]. LGGs are less aggressive and have a better prognosis than their high-grade counterparts, nonetheless, they remain incurable and impart significant negative impacts on patients' quality of life [13, 14]. Although conventional treatment approaches for cancer encompass surgical intervention, radiotherapy, and chemotherapy, recent advancements have brought forth the exploration of immunotherapies, targeted therapies, and epigenetic interventions [15–19]. Despite the expanding array of therapeutic modalities available to oncology patients, challenges such as tumor recurrence following surgical resection and the limited responsiveness of most patients to emerging therapies or development of treatment resistance persist, presenting significant hurdles in cancer management [20, 21]. Consequently, there is an urgent imperative to actively pursue alternative therapeutic targets and novel, highly sensitive tumor biomarkers, with the aim of unveiling innovative treatment strategies.

Sustained DNA damage in cells triggers repair pathways for cell survival, and the sort of DNA damage determines which repair pathways are activated [22]. X-ray repair cross-complementing 1 (XRCC1), a vital DNA repair scaffold, interacts closely with DNA ligase IIIα (Lig-III) to orchestrate the mending of DNA single-strand breaks triggered by ionizing radiation and alkylating agents, encompassing the base excision repair (BER) and single-strand break repair (SSBR) pathways [23, 24]. The BER pathway maintains genomic integrity and stability [25], with XRCC1 playing a critical role as a DNA repair gene by acting as a backbone protein in the initial and late steps of this pathway [26]. XRCC1 exhibits differential expression patterns across various normal human tissues, with slightly elevated levels observed in gonadal tissues and comparatively lower levels in pancreatic tissues [27]. In the context of tumorigenesis, XRCC1 manifests distinct expression profiles in different cancer tissues and serves as a valuable biological marker for tumors. Notably, nuclear expression levels of XRCC1 demonstrate associations with the prognosis of patients with biliary tract cancer and provide predictive insights into therapeutic responses following chemotherapy [28]. Intriguingly, gliomas exhibit reduced XRCC1 expression compared to normal tissues and augmented XRCC1 expression significantly impedes malignant

biological behaviors [29]. Noteworthy regulatory mechanisms governing XRCC1 functionality include epigenetic modifications, gene mutations, and phosphorylation alterations. Methylation events involving XRCC1 have been linked to sperm chromatin condensation in males and sperm DNA fragmentation in patients with idiopathic oligospermia [30]. Gastric cancer tissues exhibit substantially higher levels of XRCC1 gene promoter methylation compared to adjacent normal tissues, with the hypermethylation status of this gene promoter significantly associated with protein expression loss [31]. Impairment in phosphorylation sites T358 and T367 on XRCC1 hampers its recruitment to DNA damage sites [32]. Additionally, phosphorylation of XRCC1 activates the microhomology-mediated end joining (MMEJ) pathway involved in DNA double-strand break repair, and MMEJ has been implicated in genomic rearrangements and oncogenic transformations [33].

In this study, we aimed to perform a comprehensive pan-cancer analysis of XRCC1, a pivotal gene in DNA repair, which has not been reported previously. To achieve this, we utilized multiple databases, including CCLE, CPTAC, HPA, GEO, TCGA, cBioPortal, TISIDB, TIMER, and XCELL. Our analysis aimed to examine XRCC1 expression levels across diverse cancer types and elucidate its prognostic implications. Furthermore, we explored the potential connections between XRCC1 expression and DNA methylation patterns, tumor mutational load (TMB), microsatellite instability (MSI), and immune infiltration levels in various cancer contexts. Through XRCC1 coexpression analysis and enrichment analysis, we sought to unravel the biological functions of XRCC1 in tumorigenesis. Remarkably, our findings identified XRCC1 as a novel prognostic and immunological biomarker, holding promise as a molecular target in numerous cancer types, with particular significance in LGGs. This analysis represents a rare and comprehensive approach in cancer research, harnessing genomic data from multiple cancer types to yield more comprehensive and precise outcomes.

MATERIALS AND METHODS

Patient data sets

To acquire the required RNAseq data, we accessed UCSC XENA (https://xenabrowser.net/datapages/) and retrieved the data in TPM (transcripts per million reads) format, which had undergone uniform processing by the Toil process [34]. For the TCGA and GTEx datasets, we performed log2 transformation on the TPM data to facilitate subsequent analysis and comparison. To conduct ROC (Receiver Operating Characteristic)

analysis of XRCC1, we employed the pROC package (v.1.17.0.1) and ggplot2 package (v3.3.3) in R (v.3.6.3). Additionally, we obtained cell line gene expression matrices of tumors from the CCLE dataset (https://portals.broadinstitute.org/ccle/about). All the aforementioned analyses were implemented using the ggplot2 package (v3.3.3) in R (v4.0.3).

Human Protein Atlas analysis

We utilized the Human Protein Atlas (https://www.proteinatlas.org/) as a valuable resource for accessing proteomic and transcriptomic data encompassing diverse human samples, including cellular, tissue, and pathological profiles. Leveraging this online database, we investigated the expression patterns of the XRCC1 gene across a range of tumor types.

Survival analysis

To analyze RNA-seq expression data from a substantial number of tumor and normal samples, we employed the GEPIA database (http://gepia.cancer-pku.cn/) [35]. This online resource encompasses a vast collection of 9736 tumor samples and 8587 normal samples obtained from the TCGA and GTEx projects. Utilizing the "Survival Map" module within GEPIA, we accessed the OS (Overall Survival) and DFS (Disease-Free Survival) significance map data for XRCC1 across a broad spectrum of human cancers. The expression thresholds of cutoff-high (50%) and cutoff-low (50%) were utilized to stratify samples into high-expression and low-expression groups. Hypothesis testing was conducted using the log-rank test, and survival plots were obtained through the "Survival Analysis" module of GEPIA. Furthermore, we performed univariate Cox regression analysis of XRCC1 expression, specifically evaluating progression-free survival (PFS) and disease-specific survival (DSS) in tumor patients. The "forest plot" R package was employed to present P-values, hazard ratios (HR), and 95% confidence intervals (CI) for each variable of interest.

UALCAN database analysis

The UALCAN database (http://ualcan.path.uab.edu/analysis-prot.html) [36] offers an interactive platform for conducting comprehensive analyses of TCGA gene expression data. Within this database, we utilized the CPTAC dataset [37] to examine protein expression and phosphoprotein levels. Furthermore, we employed the UALCAN database's coverage of the TCGA dataset to investigate the methylation levels of XRCC1 DNA across various cancer types. Statistical analysis was conducted using Student's t-test to assess the significance of differences, with a p-value threshold of less than 0.05 considered statistically significant.

Pan-cancer analysis of genetic alterations of XRCC1

The cBio Cancer Genomics Portal (cBioPortal) (http://cbioportal.org) [38] is a valuable resource for exploring, visualizing, and analyzing multidimensional cancer genomics data. In our study, we leveraged the cBioPortal database to investigate the mutation frequency, mutation types, copy number alterations (CNAs), and mutation sites of XRCC1 across all TCGA tumors. Furthermore, we examined the potential relationship between genetic alterations in XRCC1 and prognosis in patients with different cancer types. Additionally, TMB and MSI scores were obtained from the TCGA dataset, and we performed correlation analysis, employing Spearman's rank correlation coefficient, to assess the association between XRCC1 expression and TMB as well as MSI.

TISIDB database analysis

The TISIDB database (http://cis.hku.hk/TISIDB/index.php) [39] serves as a comprehensive web portal focusing on tumor and immune system interactions, encompassing diverse data types. In our investigation, we utilized the TISIDB database to explore the correlations between XRCC1 expression and immune or molecular subtypes in various cancer types. Statistical significance was determined with a p-value threshold of less than 0.05, indicating meaningful differences in the observed associations.

Correlation analysis of XRCC1 expression with immune infiltrating cells and their marker genes

We obtained data for 33 cancers and normal tissues from the Genomic Data Commons (GDC) [40] data portal within the TCGA database. To ensure an accurate assessment of immune correlations, we utilized the immunedeconv R package, which integrates six advanced algorithms: TIMER, XCELL, CIBERSORT, EPIC, MCPCOUNTER, and QUANTISEQ. The generated heat map depicts different types of cancer on the horizontal axis, various immune scores on the vertical axis, and correlation coefficients represented by distinct colors. Additionally, we explored the relationship between XRCC1 expression in immune cells and multiple markers using the TIMER database (http://cistrome.org/TIMER/) [41]. The x-axis displays XRCC1 expression levels, while the y-axis represents other relevant genes. Statistical significance is denoted by asterisks: * indicates p < 0.05, ** indicates p < 0.01, and *** indicates p < 0.001.

Correlation analysis of XRCC1 expression with immune checkpoint

To delve deeper into the analysis of the expression of 47 common immune checkpoint genes in relation to XRCC1, we employed the limma package [42]. Specifically, we extracted these immune checkpoint genes and calculated their correlation with XRCC1 expression individually. For a correlation to be considered significant, we set the thresholds at $p < 0.05$ and $R > 0.20$, indicating a statistically significant positive correlation between XRCC1 and the immune checkpoint genes.

Gene enrichment analysis and PPI network construction

We explored the differential expression genes (DEGs) between different XRCC1 expression groups (low expression group: 0–50%; high expression group: 50–100%) in LGG using the DESeq2 package. The volcano map was drawn by the ggplot2 package with the threshold values of |log2 fold-change (FC)|>1.0 and adjusted P-value<0.05. Then, we performed GO term enrichment, KEGG pathway enrichment and Gene enrichment analysis (GSEA) of DEGs using the ggplot2 package for visualization and the clusterProfiler package [43] for statistical analysis. The Tool for Interactive Gene Search (STRING) (https://string-db.org/cgi/input.pl) [44] is a public database providing protein interaction information. We used the STRING online database to construct PPI networks for 134 genes obtained at threshold |log2 fold-change (FC)|>2.0 and adjusted p-value<0.05 and screened hub gene by Cytoscape [45].

Analysis of mutations, methylation, and pathway activity of XRCC1 and its hub gene

To further expand our analysis, we utilized GSCALite (http://bioinfo.life.hust.edu.cn/web/GSCALite/) [46], which offers various analysis modules to examine multi-omics data. The database incorporates data from multiple sources, including 11,160 samples from TCGA covering 33 cancer types (TCGA Cancer), information on Cancer Drug Sensitivity Genomics with 746 drug data from the Cancer Therapeutic Response Portal, as well as 11,688 normal tissue expression data from the Genotype-Tissue Expression (GTEx) project. With the help of GSCALite, we investigated several aspects, including copy number variation (CNV), methylation patterns, pathway activity, and drug sensitivity. These analyses allow us to gain insights into the genetic alterations, epigenetic modifications, cellular pathway dynamics, and potential therapeutic responses

associated with XRCC1 and its involvement in different cancers.

Statistical analysis

In our study, R (version 3.6.3) was employed for conducting statistical analyses. The Wilcoxon signed rank sum test was utilized to investigate the expression of XRCC1 in tumor tissues and their corresponding neighboring tissues. Cox regression analysis and the Kaplan-Meier method were applied to evaluate prognostic factors. Student's test was used to compare protein expression, phosphoprotein levels, and DNA methylation levels of XRCC1 between normal and tumor groups. The correlation between XRCC1 expression and tumor mutational burden (TMB) as well as microsatellite instability (MSI) was examined using Spearman's rank correlation analysis. Furthermore, we assessed the association between XRCC1 expression and clinical-pathological characteristics of LGG using the Kruskal-Wallis and Wilcoxon rank sum tests. A p-value below 0.05 was considered statistically significant in all statistical tests performed.

Data availability statement

The datasets presented in this study can be found in online repositories. The names of the repository/repositories and accession number(s) can be found in the article Supplementary Material.

RESULTS

Pan-cancer analysis of XRCC1 differential expression and clinicopathological correlation

In this study, we aimed to investigate the role of XRCC1 in carcinogenesis. Firstly, we analyzed the expression status of XRCC1 in various tumor tissues and paired normal tissues (Figure 1A). The results revealed significantly higher expression levels of XRCC1 in tumor tissues compared to normal tissues in multiple cancer types, including bladder urothelial carcinoma (BLCA), breast invasive carcinoma (BRCA), cholangiocarcinoma (CHOL), colon adenocarcinoma (COAD), esophageal carcinoma (ESCA), head and neck adenocarcinoma (HNSC), kidney renal clear cell carcinoma (KIRC), kidney renal papillary cell carcinoma (KIRP), liver hepatocellular carcinoma (LIHC), lung squamous cell carcinoma (LUSC), pheochromocytoma and paraganglioma (PCPG), rectum adenocarcinoma (READ), and stomach adenocarcinoma (STAD). Conversely, the expression level of XRCC1 was low in the kidney chromophobe (KICH) (Figure 1A). We further validated our findings by analyzing the expression of XRCC1 in normal samples from the
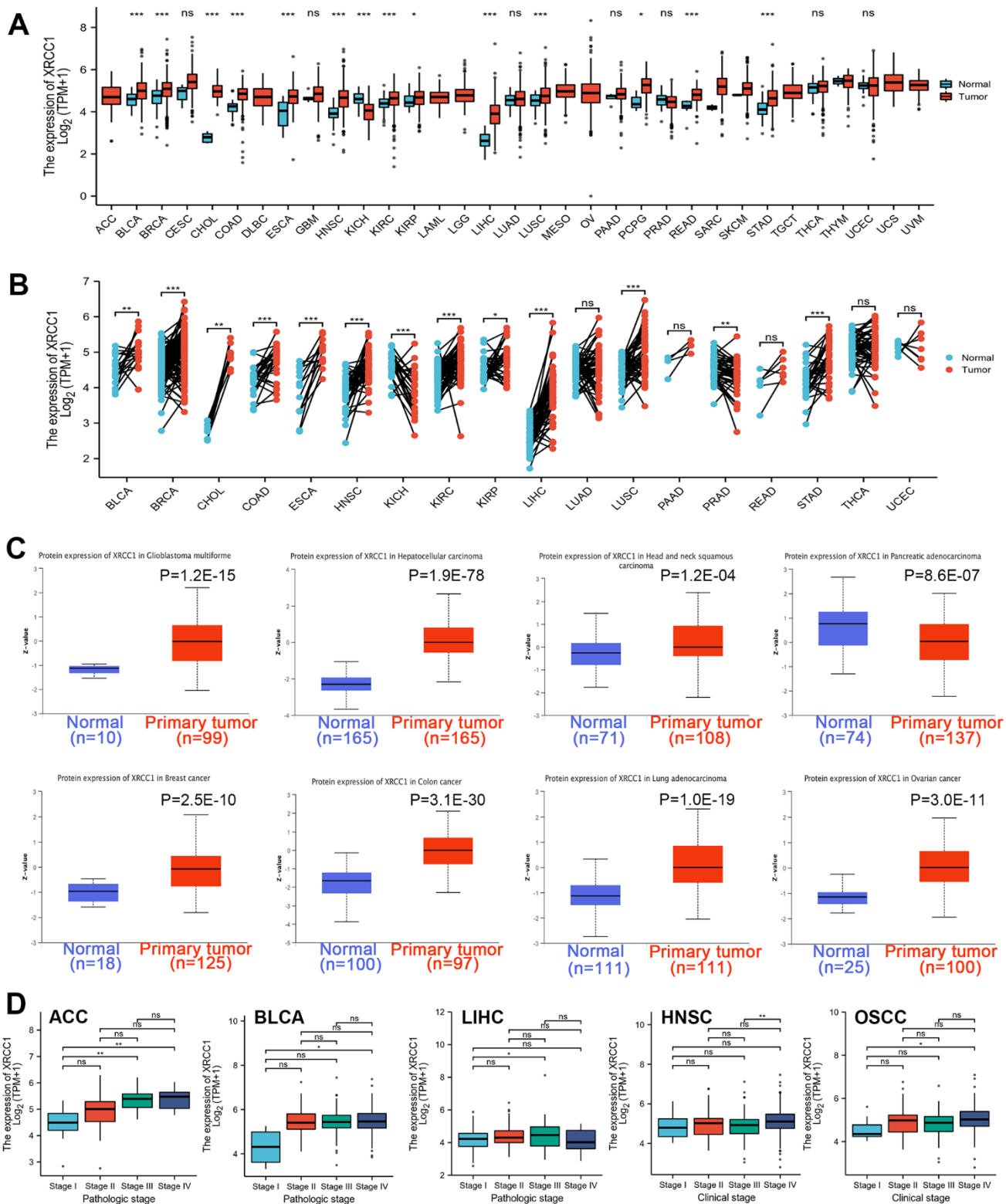
Figure 1. (**A**) Human XRCC1 gene expression status in various cancers from TCGA database. (**B**) Wilcoxon signed rank sum test was used to detect the differential expression of XRCC1 in tumor tissues and adjacent paracancerous tissues. (**C**) The protein expression level of the XRCC1 gene in glioblastoma multiforme, hepatocellular carcinoma, head and neck squamous carcinoma, pancreatic adenocarcinoma, breast cancer, ovarian cancer, colon cancer, lung adenocarcinoma, clear cell RCC. (**D**) The box plot of tumor pathological stages (stage I, stage II, stage III, stage IV) following ACC, BLCA, LIHC, and clinical stages (stage I, stage II, stage III, stage IV) of HNSC, OSCC. ns P≥0.05, *P<0.05, **P<0.01; ***P<0.001.

Genotype-Tissue Expression (GTEx) database and matched adjacent tumor tissues (Supplementary Figure 1A). To assess the expression of XRCC1 in tumor tissues compared to their matched adjacent tissues, we performed the Wilcoxon signed rank sum test (Figure 1B). Moreover, we explored the expression of XRCC1 in a broader range of cancer tissues using the Cancer Cell Line Encyclopedia (CCLE) database, which provided cell line expression matrices for various tumor types (Supplementary Figure 1B). To examine the protein expression of XRCC1, we utilized the Clinical Proteomic Tumor Analysis Consortium (CPTAC) database. Our analysis demonstrated significantly higher protein expression levels of XRCC1 in primary tissues of GBM, hepatocellular carcinoma, head and neck squamous carcinoma, breast cancer, colon cancer, lung adeno-carcinoma (LUAD), and ovarian cancer compared to normal tissues (Figure 1C). Additionally, we provided supplemental protein expression data for XRCC1 genes that did not show significant differences (Supplementary Figure 1C). These findings were further confirmed using the Human Protein Atlas (HPA) database (Supplementary Figure 2). Finally, we investigated the association between XRCC1 gene expression and clinical characteristics. We assessed XRCC1 expression levels in different tumor stages of Adrenocortical carcinoma (ACC), BLCA, and LIHC. Furthermore, we examined the correlation between XRCC1 expression and clinical stages in head and neck squamous cell carcinoma (HNSC) and oral squamous cell carcinoma (OSCC) (Figure 1D). Additionally, we analyzed the differential expression of XRCC1 based on patient age, gender, T-stage, and histological grade (Supplementary Figure 3).

Pan-cancer analysis of the multifaceted prognostic value of XRCC1

We separated the cancer cases into low-expression and high-expression groups based on the gene expression levels of XRCC1. We explored the relativity between XRCC1 gene expression levels and the survival prognosis across cancer types with the assistance of GEO and TCGA datasets. According to Figure 2A, high XRCC1 gene expression was related to poor overall survival (OS) in cancers of acute myeloid leukemia (LAML) (n=106, P=0.041) and LGG (n=514, P=0.011) in the TCGA dataset. Disease-free survival (DFS) relevant statistics in Figure 2B revealed a linkage between poor prognosis and high XRCC1 gene expression levels for the cancer cases from the TCGA dataset of LGG (n=521, P=0.024), LIHC (n=364, P=0.0053) and LUAD (n=478, P=0.034). Meanwhile, high expression of the XRCC1 gene was linked to better DFS in GBM (n=160, P=0.012) and thymoma (THYM) (n=118, P=0.019). In summary, we found that the gene expression level of XRCC1 was mainly relevant to the poor survival prognosis of patients

with various cancer types. Furthermore, we conducted a survival relevance analysis across multiple cancer types, including progression-free survival (PFS) and disease-specific survival (DSS), to learn the relevance of XRCC1 gene expression levels to the survival prognosis of cancer patients. The forest plot of PFS analysis indicated that higher XRCC1 gene expression levels were relevant to worse PFS in ACC (P=0.0171), LGG (P <0.0001) and LUAD (P= 0.0268), whereas better PFS in BRCA(P=0.0429) (Figure 3A). Furthermore, analysis of DSS prognosis (Figure 3B) showed the relevance of higher XRCC1 gene expression levels to worse DSS in patients with cervical squamous cell carcinoma and endocervical adenocarcinoma (CESC) (P=0.0015), COAD (P=0.0268), KIRC (P=0.0296), LIHC (P=0.0086) and LUSC (P=0.0190). The data from other cancer types are all statistically insignificant. In summary, our findings indicate that XRCC1 gene expression levels are predominantly associated with poor survival prognosis in various cancer types. Furthermore, the analysis of PFS and DSS across multiple cancer types further supports the relevance of XRCC1 gene expression levels to the survival prognosis of cancer patients.

Diagnostic value of XRCC1 in pan-cancer

In our analysis, we utilized receiver operating characteristic (ROC) curves to assess the predictive ability of XRCC1 expression levels in distinguishing between cancer and normal tissue across multiple cancer types. The results demonstrated that XRCC1 exhibited a considerable accuracy (AUC>0.7) in predicting 20 cancer types, including ACC (AUC= 0.789), BLCA (AUC=0.708), BRCA (AUC=0.763), CESC (AUC=0.776), CHOL (AUC=1.000), COAD (AUC=0.787), DLBC (AUC=0.787), ESCA (AUC= 0.757), GBM (AUC=0.828), HNSC (AUC=0.857), KIRC (AUC=0.731), KIRP (AUC=0.746), LGG (AUC=0.847), LIHC (AUC=0.933), OSCC (AUC= 0.851), PAAD (AUC=0.965), READ (AUC=0.770), SKCM (AUC=0.862), STAD (AUC=0.813), and THYM (AUC=0.945) (Figure 4). Notably, XRCC1 exhibited high accuracy (AUC>0.9) in predicting CHOL, LIHC, PAAD, and THYM. These findings suggest that XRCC1 has the potential to serve as an excellent biomarker for cancer diagnosis. Supplementary Figure 4 provides the ROC curves for XRCC1 in other cancer types for reference.

Pan-cancer analysis of the phosphorylation of XRCC1

In our analysis, we investigated the differences in XRCC1 protein expression and phosphorylation between primary tumor tissues and normal tissues. Utilizing the CTPAC database, we focused on nine

types of tumors, namely breast cancer, ovarian cancer, COAD, RCC, UCEC, LUAD, GBM, PAAD, and HNSC. Initially, we examined the XRCC1 protein phosphorylation sites and identified notable differences (Figure 5A). Specifically, the phosphorylation level at the T453 locus within the XRCC1 protein was significantly elevated in breast cancer, colon cancer, LUAD, UCEC, and pancreatic adenocarcinoma compared to normal tissues (all P < 0.05) (Figure 5B, 5D, 5E, 5G, 5H). Furthermore, we observed an increased phosphorylation level at the S241 locus within XRCC1 protein in breast cancer (P = 9.4E-13), colon cancer (P = 1.7E-34), GBM (P = 4.4E-02), UCEC (P = 7.4E-20), and ovarian cancer (P = 1.1E-08) (Figure 5B, 5D, 5F, 5G, 5I). These findings indicate the potential significance of phosphorylation events in tumorigenesis. Further molecular assays are warranted to gain a deeper understanding of the role of phosphorylation at these specific loci in various types of cancer development.
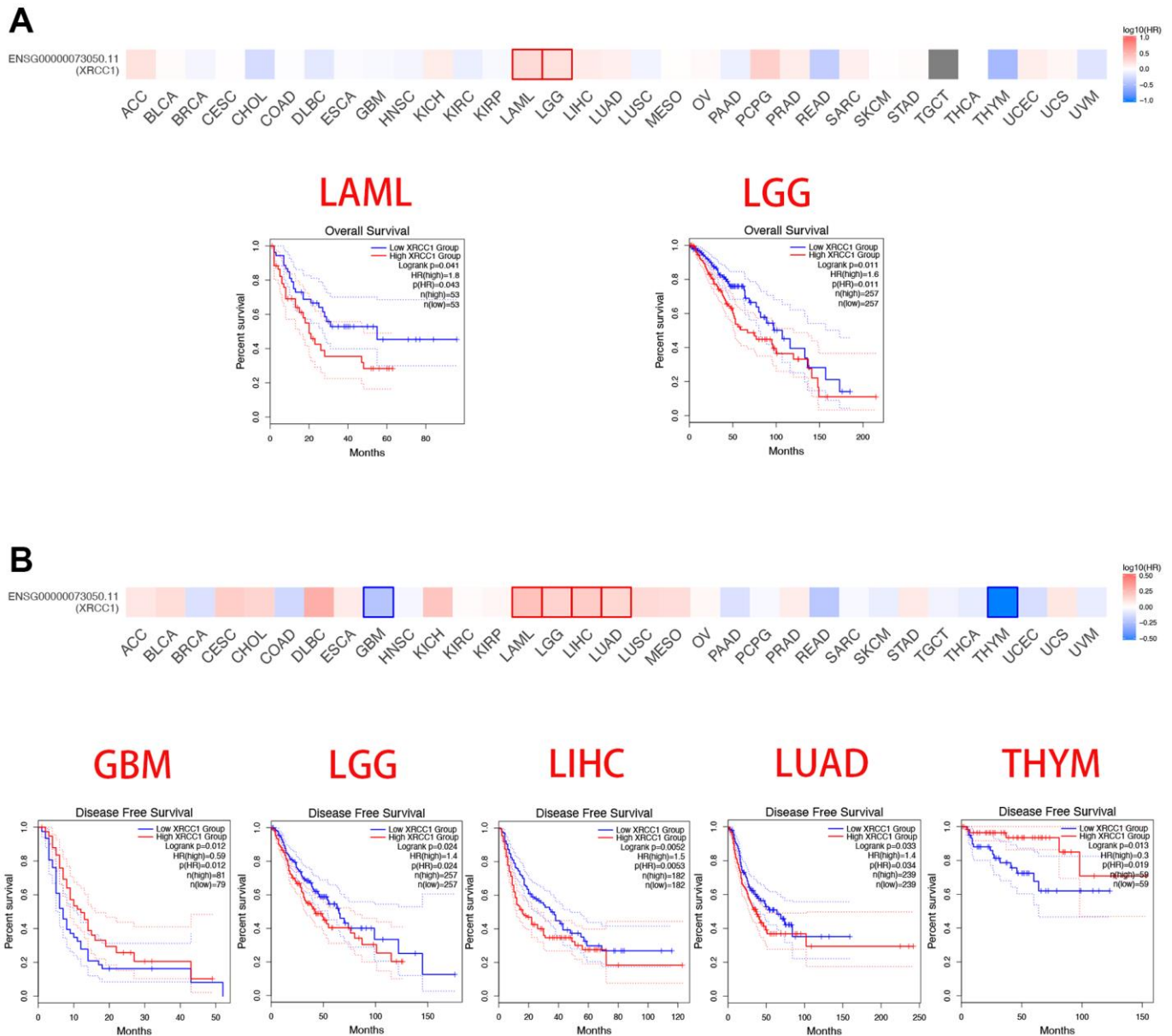

Figure 2. Summary of relativity between survival prognosis across cancer types in TCGA dataset and XRCC1 gene expression levels. The GEPIA database was utilized to plot overall survival (**A**) and disease-free survival (**B**) conditions across cancer types in TCGA dataset by XRCC1 gene expression. We observed that high XRCC1 gene expression was related to worse OS and DFS in almost all cancer types, except DFS in UCEC cohorts(n=160) and THYM cohorts(n=118). Only p-values < 0.05 were displayed.

Pan-cancer analysis of the methylation level and genetic alteration of XRCC1

We conducted an analysis of XRCC1 genomic alterations in pan-cancer using the cBioPortal (TCGA, The Pan-Cancer Atlas) database. Our findings revealed that genomic alterations in XRCC1 were detected in 1.8% of patients (Figure 6A). Further exploration of the genetic alteration status of XRCC1 in different tumor samples within the TCGA cohort showed distinct patterns. Among these, the highest frequency of alterations in XRCC1 (>6%) was observed in patients with uterine carcinosarcoma (UCS), where "Amplification" was the predominant type of alteration (Figure 6B). In cases of DLBC with genetic alterations, copy number deletion of XRCC1 was the prevalent type of alteration. Notably, the "Structural Variant" type of XRCC1 alteration was exclusively found in cases of LUSC. Furthermore, we analyzed the types, sites, and cases of XRCC1 genetic alterations. Missense mutations were the most common type of alteration, and specific alterations such as P333L/T in the BRCT
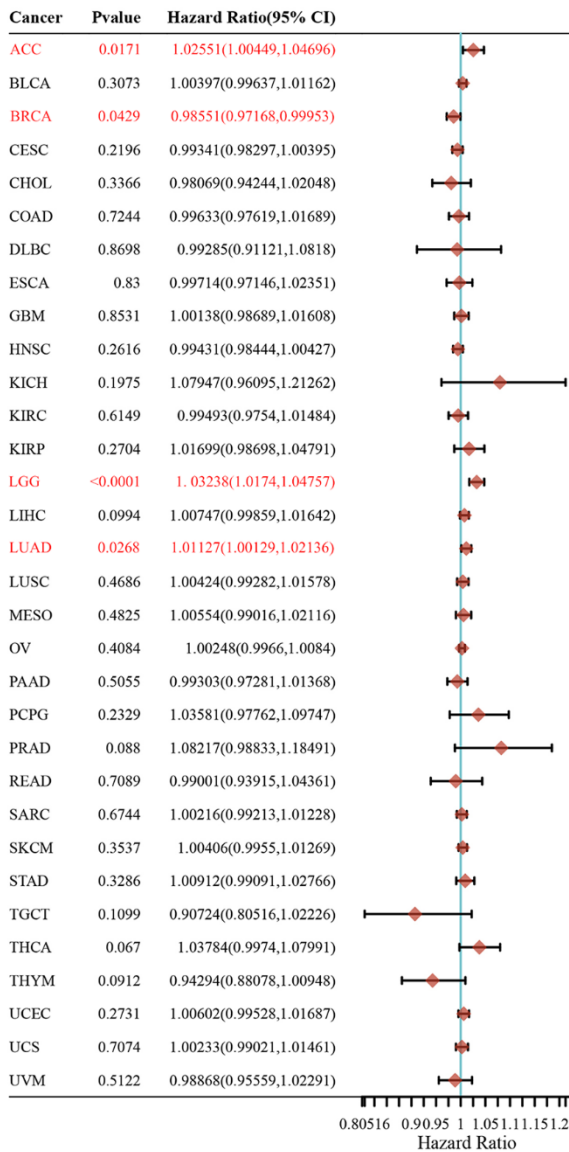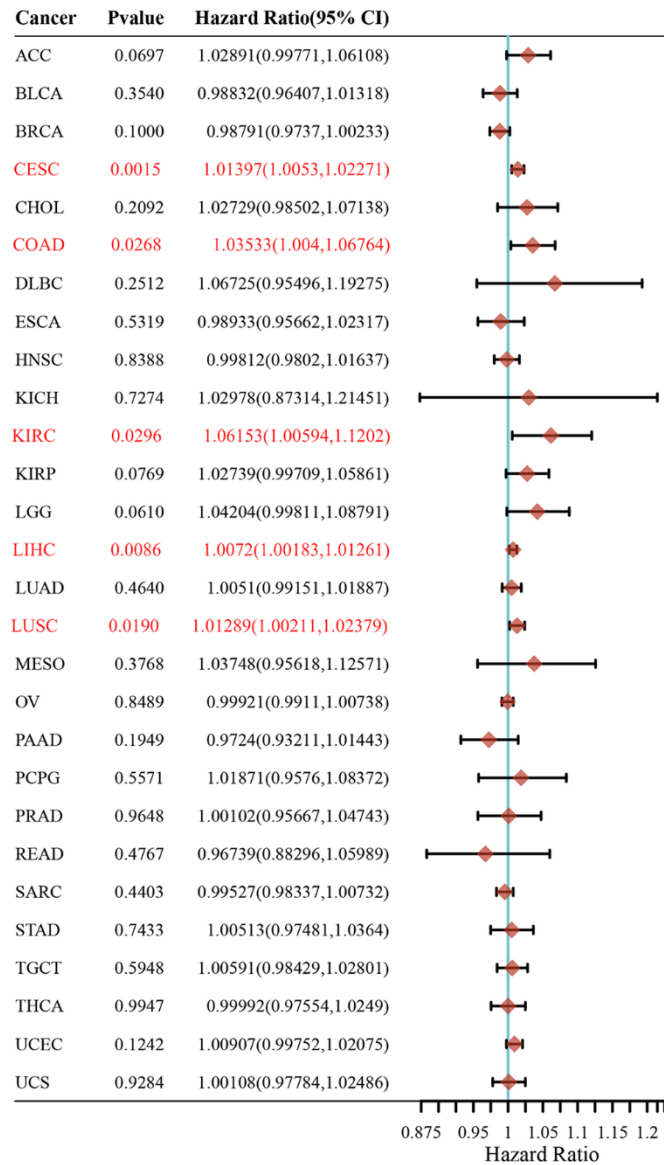

Figure 3. Association between XRCC1 expression levels and cancer patients' PFS and DSS prognosis, using univariate survival analysis in various cancers. (**A**) Relevance of XRCC1 gene expression levels to PFS prognosis across cancer types in TCGA dataset. (**B**) Relevance of XRCC1 gene expression to DSS prognosis across cancer types in TCGA dataset. Red font indicated P-value < 0.05.
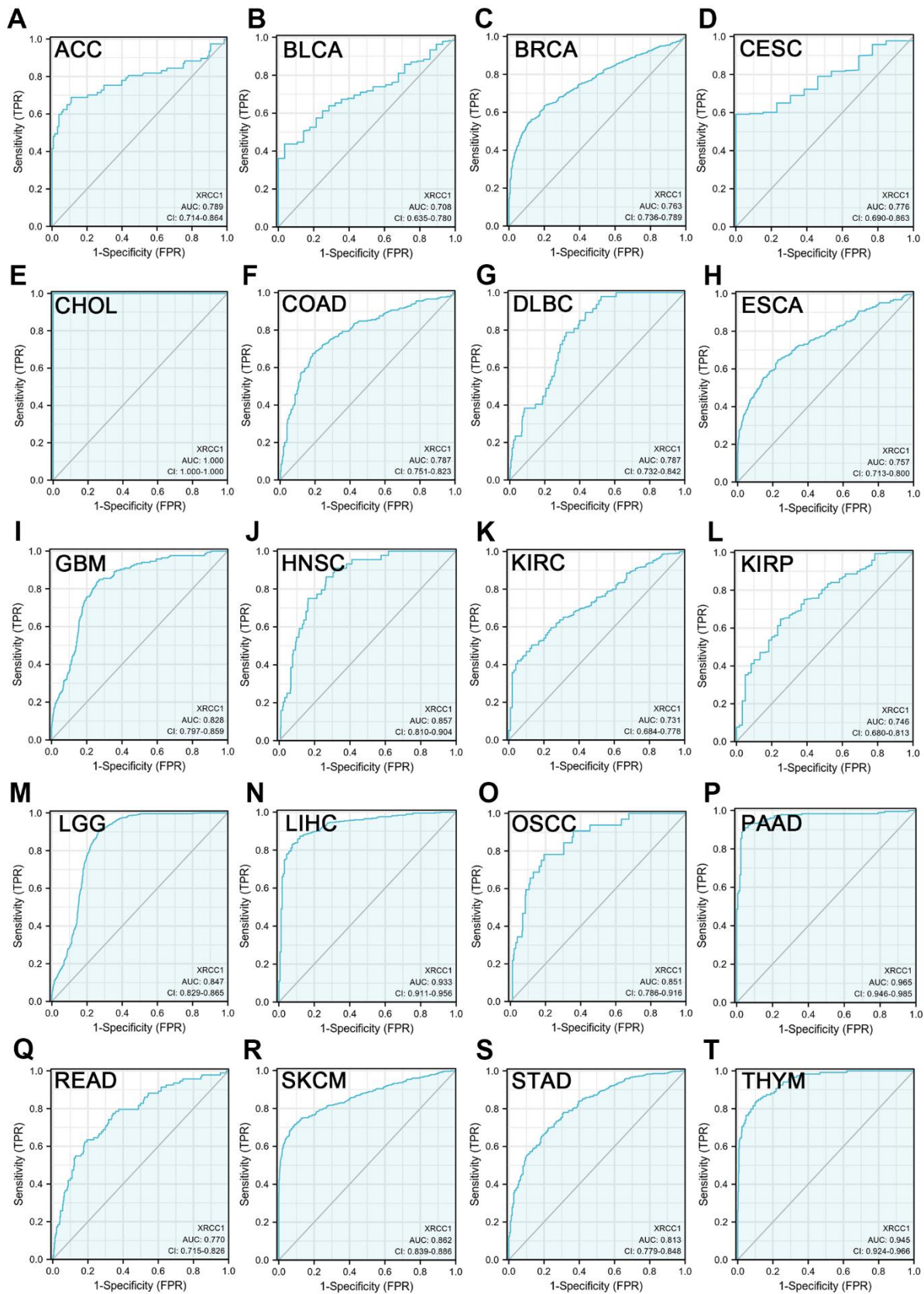
Figure 4. XRCC1 expression levels could distinguish between cancerous and normal tissues in pan-cancer. (**A**) ACC; (**B**) BLCA; (**C**) BRCA; (**D**) CESC; (**E**) CHOL; (**F**) COAD; (**G**) DLBC; (**H**) ESCA; (**I**) GBM; (**J**) HNSC; (**K**) KIRC; (**L**) KIRP; (**M**) LGG; (**N**) LIHC; (**O**) OSCC; (**P**) PAAD; (**Q**) READ; (**R**) SKCM; (**S**) STAD; (**T**) THYM. X-axis reveals the false positive rate, while Y-axis indicates the true positive rate.
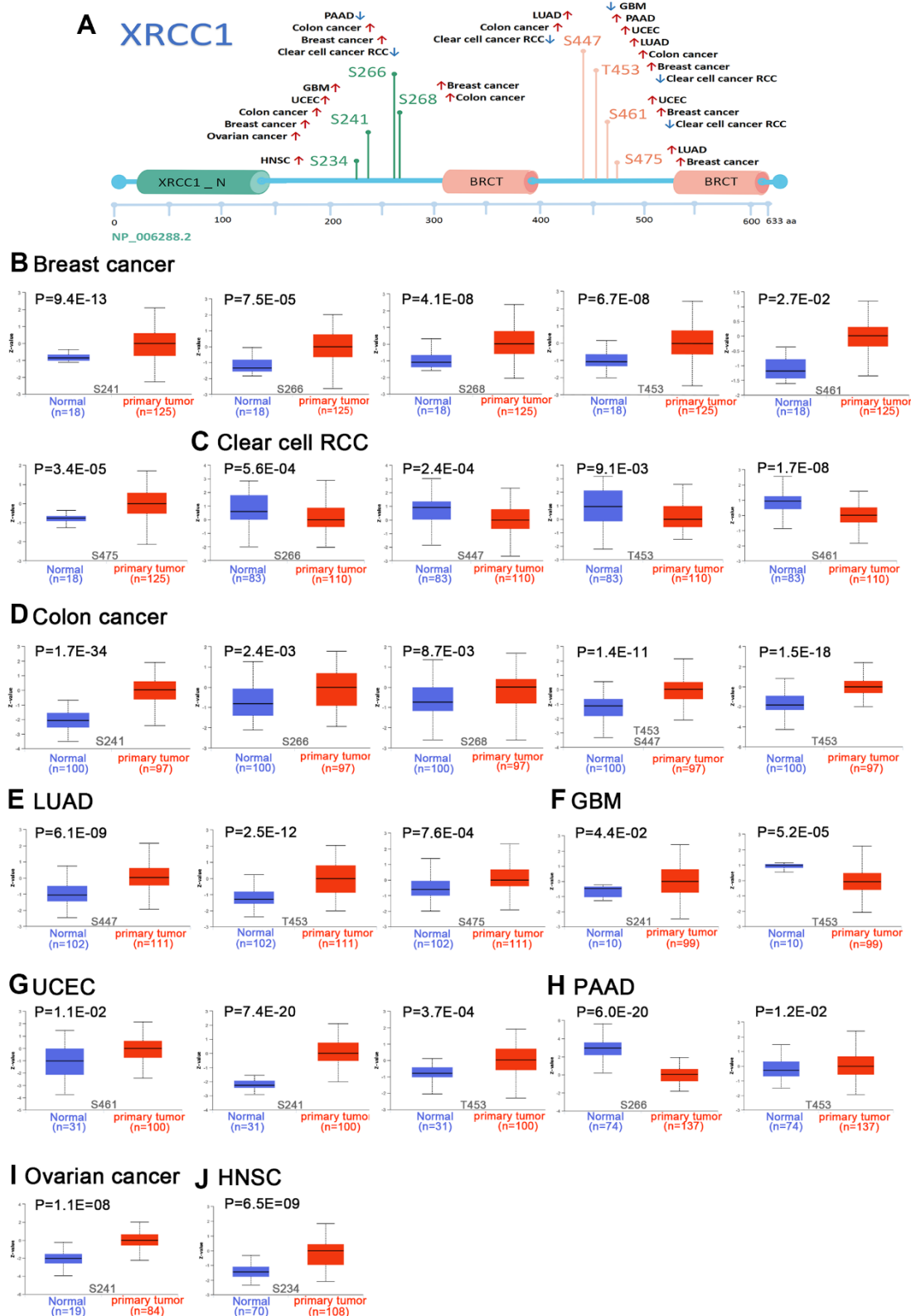
Figure 5. We utilized the UALCAN tool to compare the expression status of XRCC1 phosphoprotein (NP_006288.2, S234, S241, S266, S268, S447, S461, S475, and T453 sites) between primary tissue of specific tumors and normal tissue from CPTAC database. The schematic diagram of XRCC1 protein (**A**) demonstrated the phosphoprotein sites with positive results. We also enriched the box plots with different tumors containing breast cancer (**B**), clear cell RCC (**C**), COAD (**D**), LUAD (**E**), GBM (**F**), UCEC (**G**), PAAD (**H**), ovarian cancer (**I**), HNSC (**J**).
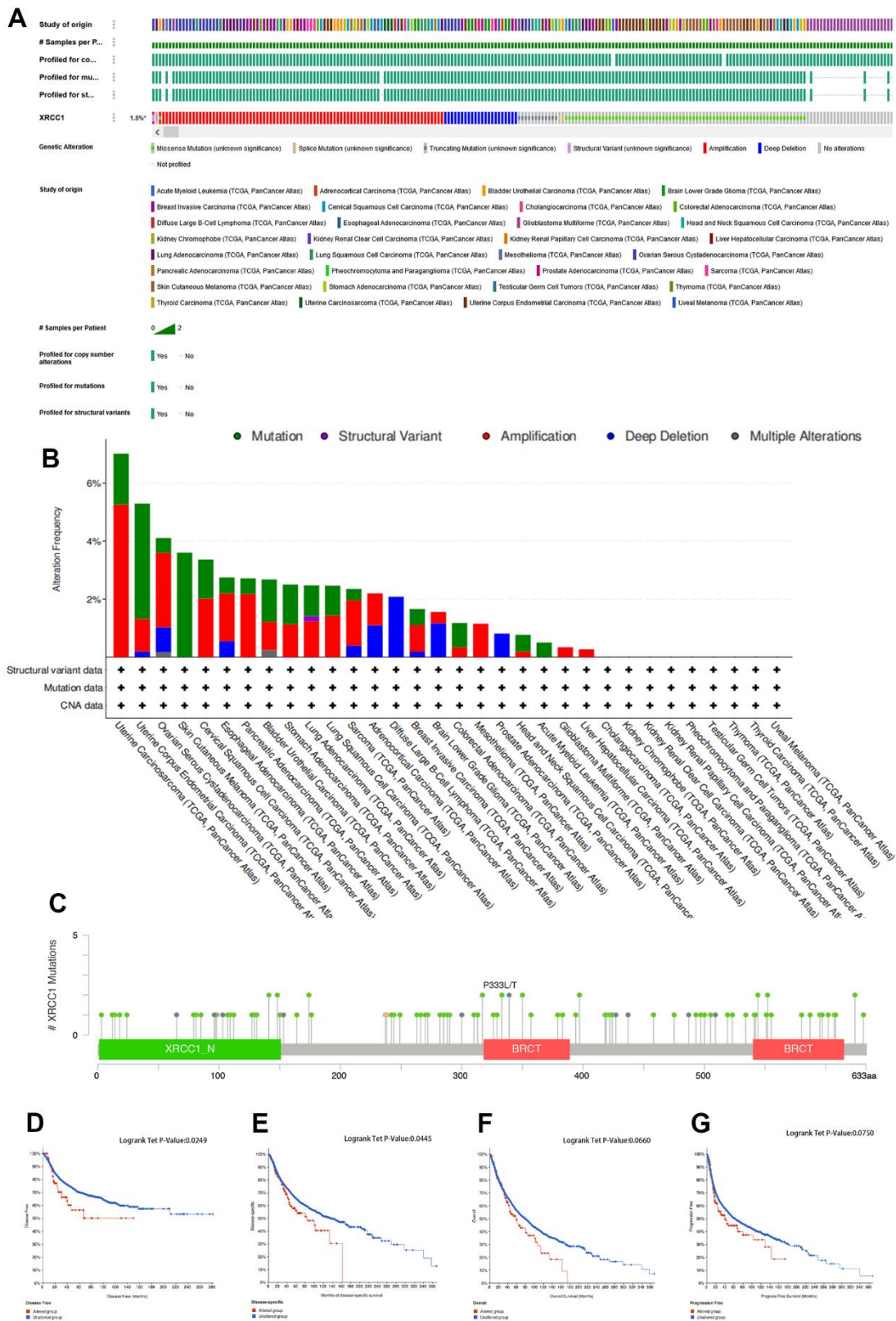
Figure 6. Mutation feature of XRCC1 in pan-cancer of TCGA. (**A**) The cBioPortal database was used to analyze the proportion of patients with XRCC1 genomic alterations in pan-cancer. The frequency of mutation type (**B**) and mutation site (**C**) of XRCC1 in TCGA tumors was analyzed using the cBioPortal tool. The cBioPortal database was used to explore the impact of XRCC1 mutation status on OS (**D**), DFS (**E**), PFS (**F**), and DSS (**G**) of cancer patients.

structural domain were identified in OV and ESCA cases (Figure 6C). Additionally, we investigated the potential association between XRCC1 genetic alterations and patient prognosis across different cancer types. The results demonstrated that patients with tumors harboring XRCC1 gene alterations exhibited poorer disease-free survival (DFS) and disease-specific survival (DSS) compared to those without alterations. Although overall survival (OS) and progression-free survival (PFS) did not reach statistical significance in the analysis between the two groups, a similar trend was observed (Figure 6D). Furthermore, we utilized the UALCAN database to analyze XRCC1 DNA methylation levels. The analysis revealed significant reductions in XRCC1 DNA methylation levels in COAD, ESCA, KIRC, KIRP, LUSC, PAAD, and SARC tissues compared to normal tissues. Conversely, elevated levels of XRCC1 DNA methylation were observed in BRCA and READ (Figure 7A). However, no significant differences in XRCC1 DNA methylation levels were observed in other tumor tissues compared to their matched normal tissues (Supplementary Figure 5).

Pan-cancer analysis of TMB and MSI of XRCC1

The study also investigated the association between XRCC1 gene expression levels and two significant biomarkers related to immunotherapy response: tumor mutational burden (TMB) and microsatellite instability (MSI). The results indicated that XRCC1 gene expression levels were significantly correlated with TMB status in several cancer types, including SARC, LUSC, UCS, and DLBC. Among these, LUSC showed particularly strong statistical significance (Figure 8A), suggesting a potential role of XRCC1 in modulating TMB in this cancer type. Furthermore, the relationship between XRCC1 gene expression levels and MSI status was explored across multiple human cancers. The analysis revealed positive correlations

between XRCC1 expression and MSI status in ACC, LGG, PAAD, MESO, and BLCA. On the other hand, BRCA and THYM showed negative correlations between XRCC1 expression and MSI status. It is worth noting that the p-value for BRCA was smaller than that of other cancers, indicating a potentially significant association (Figure 8B). These findings suggest that XRCC1 gene expression levels may be linked to the underlying genomic instability and DNA repair processes associated with TMB and MSI in various cancer types.

Pan-cancer analysis of immune and molecular subtypes of XRCC1

The study conducted an analysis of XRCC1 expression in relation to immune subtypes and molecular subtypes of human cancer using the subtype module of the TISIDB database. Immune subtypes were classified into six types: C1 (wound ranging), C2 (IFN-gamma dominant), C3 (inflammatory), C4 (lymphocyte depleted), C5 (immunologically quiet), and C6 (TGF-B dominant). The analysis revealed significant differences in XRCC1 expression among different immune subtypes in multiple cancer types, including BLCA, BRCA, COAD, ESCA, HNSC, KIRC, LGG, LIHC, LUAD, PAAD, PCPG, PRAD, SARC, STAD, TGCT, and UCS (Figure 9). Additionally, XRCC1 expression displayed significant differences among different molecular subtypes in several cancer types, including BRCA, GBM, HNSC, KIRP, LGG, LIHC, OV, PCPG, READ, STAD, and UCEC (Figure 10). XRCC1 expression in different immune and molecular subtypes of other cancers is shown in Supplementary Figure 6. These findings indicate that XRCC1 expression varies significantly across different immune and molecular subtypes in various human cancer types, highlighting the potential involvement of XRCC1 in distinct tumor microenvironments and molecular pathways.
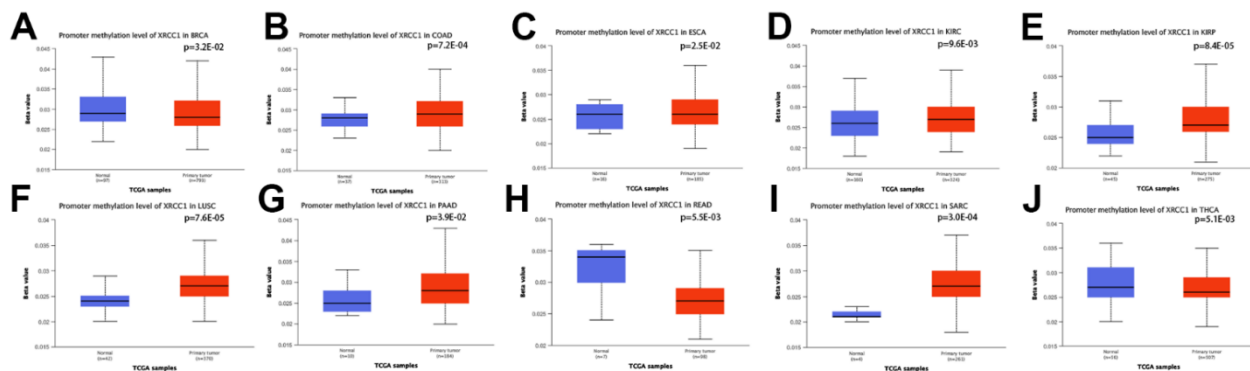

Figure 7. Promoter methylation level of XRCC1 in pan-cancer. (**A**) in BRCA, (**B**) in COAD, (**C**) in ESCA, (**D**) in KIRC, (**E**) in KIRP, (**F**) in LUSC, (**G**) in PAAD, (**H**) in READ, (**I**) in SARC, (**J**) in THCA.

Pan-cancer analysis of the XRCC1 expression and immune cell infiltration

The study utilized the TIMER and XCELL datasets to investigate the correlation between XRCC1 expression and immune infiltration in multiple tumor tissues. The results demonstrated significant correlations between XRCC1 expression and the abundance of infiltrating immune cells in various cancer types. Specifically, XRCC1 expression showed significant correlations with T cell CD8+ infiltration in 15 types of cancer, T cell CD4+ infiltration in 14 types of cancer, neutrophil infiltration in 14 types of cancer, myeloid dendritic cell infiltration in 11 types of cancer, and B cell infiltration in 9 types of cancer. The significance of these correlations was assessed using the Wilcox test (Figure 11A). Furthermore, the study employed the XCELL algorithm to explore the relationship between XRCC1 expression and the immune infiltration levels of different immune cell subtypes. The analysis revealed a

significant negative correlation between XRCC1 expression and immune infiltration in LUAD, LUSC, SARC, TGCT, THCA, and UCEC. Additionally, positive associations were observed between XRCC1 expression and common lymphoid progenitor infiltration, as well as T cell CD4+ Th1 and Th2 cell infiltration, across various cancer types (Figure 11B). Similar results were obtained using other algorithms such as CIBERSORT, EPIC, MCPCOUNTER, and QUANTISEQ (Supplementary Figure 7).

Subsequently, we investigated the correlation between XRCC1 expression status and immune cell markers in LGG through the TIMER database, involving B cell, CD8+ T cells, M1/M2 macrophages, tumor-associated macrophages (TAM), neutrophils, Natural killer cell, dendritic cells. Meanwhile, a series of functional T cells, like Th1, Th2, Th9, Th17, Th22, Tfh, exhausted T cells, Treg cells were also be examined. The outcomes suggested that XRCC1 expression was obviously
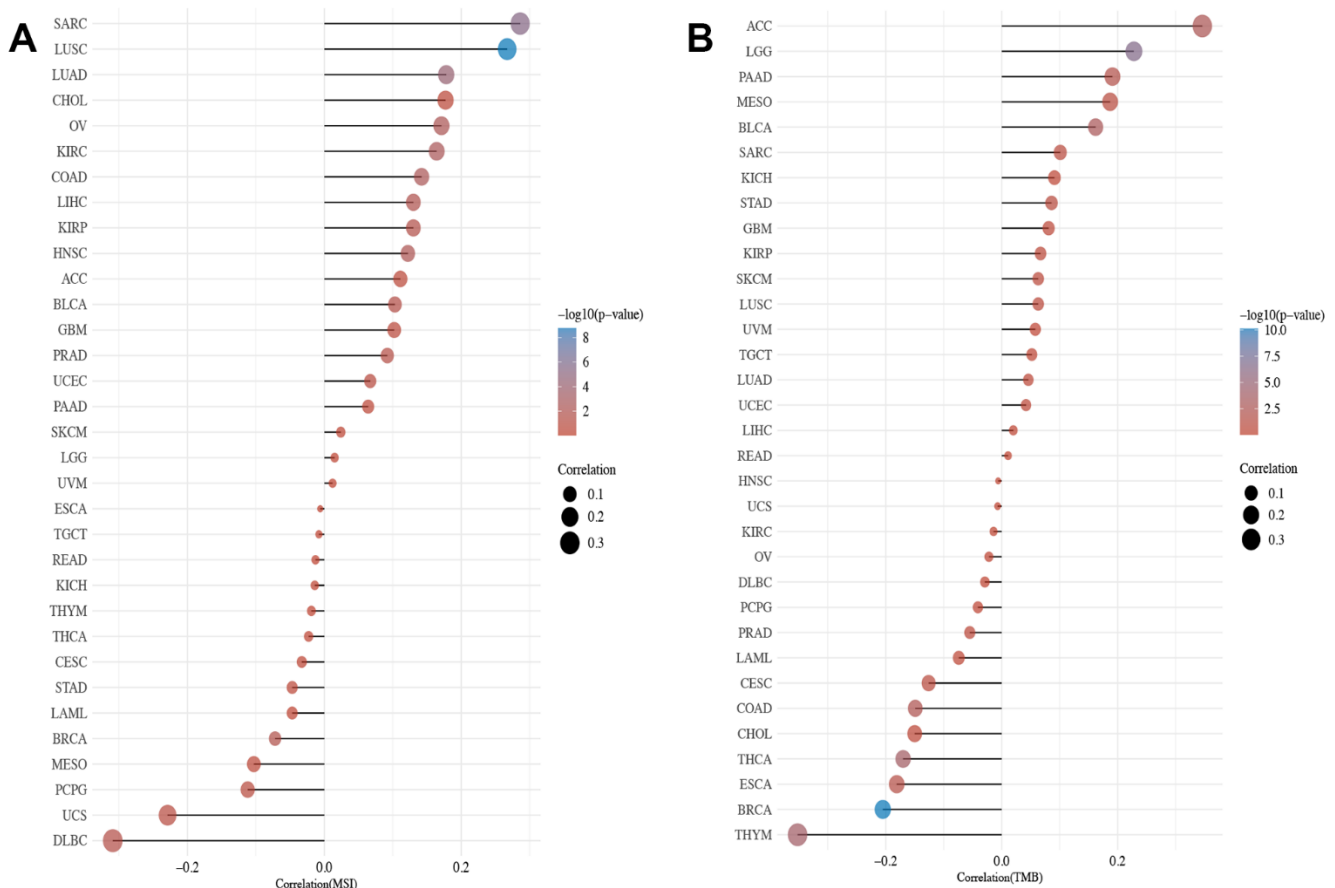
Figure 8. The relevance of XRCC1 gene expression levels to TMB and MSI across cancer types. (**A**) A bar chart reveals the relevance of XRCC1 gene expression levels to TMB in pan-cancer. (**B**) A bar chart shows the relationship between XRCC1 gene expression levels and MSI in multiple cancer types. The horizontal axis in the figure represents the correlation coefficient between genes and TMB/MSI, the ordinate is different tumors, the size of the dots in the figure represents the value of the correlation coefficient, and the different colours represent the degree of statistical significance. The bluer the colour, the smaller the p-value.

associated with the infiltration levels of immune cell markers containing B cell, Tfh, Th2, Th9, Th22, exhausted T cell, macrophage, TAM, monocyte, neutrophil and natural killer cell (Table 1).

Pan-cancer analysis of the correlation between the XRCC1 expression and immune checkpoint genes

The study evaluated the correlation between XRCC1 expression and the expression of immune checkpoint genes, which are crucial in regulating the immune response in various tumors. A total of 47 immune checkpoint genes, including both immunosuppressive and immunostimulatory genes, were analyzed in multiple cancer types (Figure 12). The results revealed a notable correlation between XRCC1 expression and

most of the immunosuppressive and immunostimulatory genes in BRCA, COAD, HNSC, LIHC, and THYM. It is worth mentioning that in HNSC, the genes showed a positive correlation with XRCC1 expression, while in COAD, they exhibited a negative correlation. These findings suggest that XRCC1 may have a role in modulating the pattern of tumor immunity by regulating the expression levels of these immune checkpoint genes in specific tumor types.

Functional enrichment analysis of XRCC1 in LGG

In the study of LGG patients, a total of 529 primary LGG cases from the TCGA database were analyzed to investigate the relationship between XRCC1 expression levels and clinicopathological characteristics (Table 2).
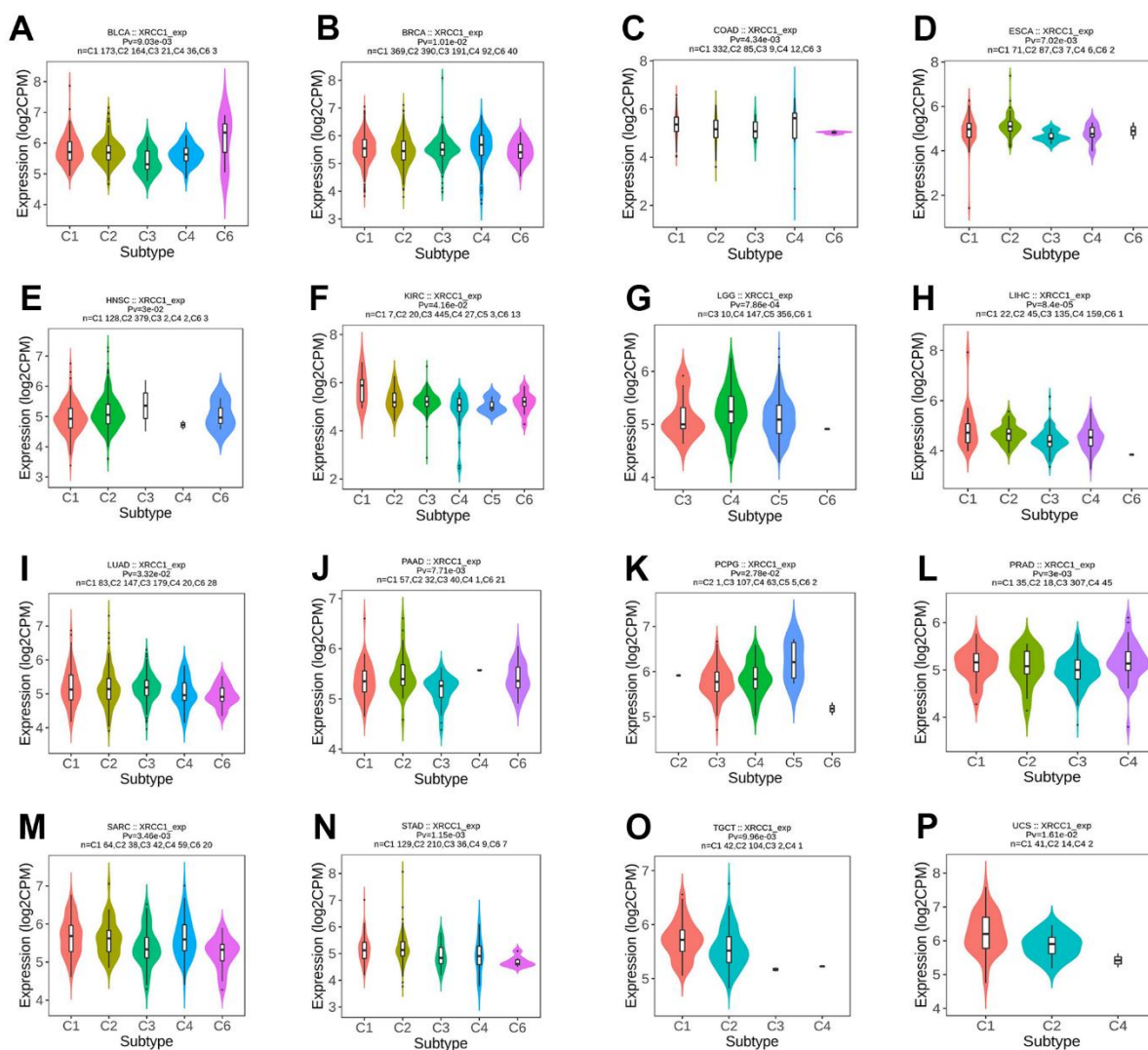

Figure 9. The relationship between XRCC1 expression and pan-cancer immune subtypes. (**A**) in BLCA, (**B**) in BRCA, (**C**) in COAD, (**D**) in ESCA, (**E**) in HNSC, (**F**) in KIRC, (**G**) in LGG, (**H**) in LIHC, (**I**) in LUAD, (**J**) in PAAD, (**K**) in PCPG, (**L**) in PRAD, (**M**) in SARC, (**N**) in STAD, (**O**) in TGCT, (**P**) in UCS.

The patients were divided into low-expression (n=264) and high-expression (n=264) groups based on the mean XRCC1 relative expression. Statistical tests such as chi-square test, Fisher's exact test, and Wilcoxon signed rank sum test were performed to analyze the associations. The results indicated significant associations between XRCC1 expression levels and several clinicopathological characteristics of LGG. XRCC1 expression was found to be correlated with WHO grade (P<0.001), IDH status (P<0.001), 1p/19q codeletion (P<0.001), and histological type (P<0.001) (Figure 13A–13D). To further confirm these findings, logistic regression analysis was conducted, and the results supported the associations between XRCC1 expression levels and the clinicopathological characteristics of LGG (Table 3). Furthermore, gene expression analysis identified a total of 1832

differentially expressed genes (DEGs) in LGG patients, including 677 upregulated genes and 1155 downregulated genes, using predefined thresholds for fold-change and adjusted p-values (Figure 13E). Among these DEGs, 134 genes exhibited significant differential expression, including 94 upregulated genes and 40 downregulated genes. Gene Ontology (GO) and KEGG pathway enrichment analyses were performed to explore the functional implications of these DEGs (Figure 13F and Supplementary Table 1). The GO analysis revealed that the DEGs were enriched in biological processes (BP) such as mitotic sister chromatid segregation, mitotic nuclear division, spindle checkpoint, DNA conformation change, and mitotic cell cycle checkpoint. In terms of cellular component (CC), the enriched categories included transmembrane transporter complex, neuron projection
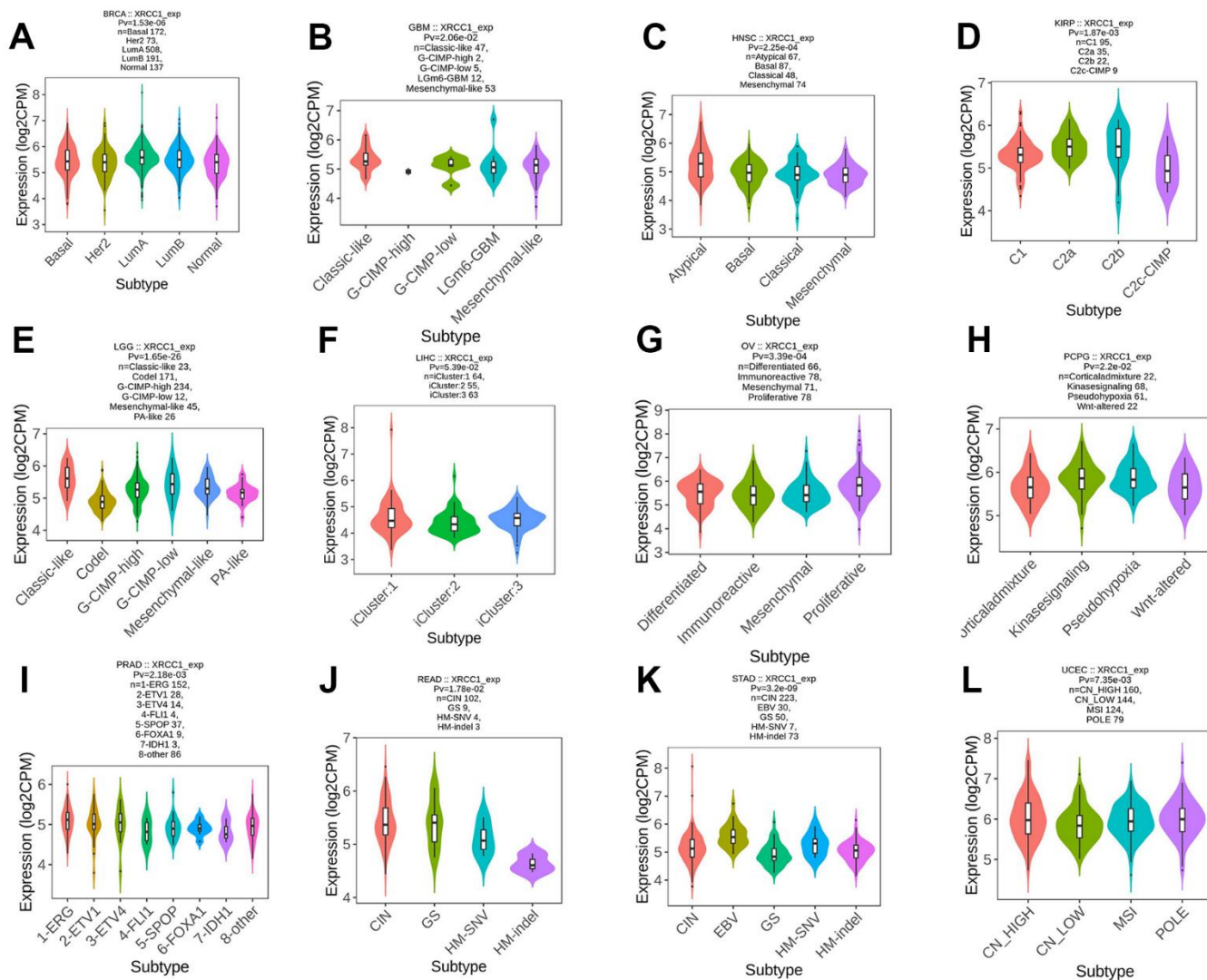

Figure 10. The relationship between XRCC1 expression and pan-cancer molecular subtypes. (**A**) in BRCA, (**B**) in GBM, (**C**) in HNSC, (**D**) in KIRP, (**E**) in LGG, (**F**) in LIHC, (**G**) in OV, (**H**) in PCPG, (**I**) in PRAD, (**J**) in READ, (**K**) in STAD, (**L**) in UCEC.

terminus, mitotic spindle, chromosomal region, and spindle microtubule. The molecular function (MF) analysis highlighted neurotransmitter receptor activity, postsynaptic neurotransmitter receptor activity, gated channel activity, microtubule binding, and histone kinase activity. Additionally, the KEGG pathway analysis revealed significant associations with GABAergic synapse, neuroactive ligand-receptor interaction, cAMP signaling pathway, cell cycle, and Ras signaling pathway. These findings provide valuable insights into the molecular characteristics and functional pathways associated with XRCC1 expression in LGG patients, shedding light on its potential role in LGG progression and suggesting potential therapeutic targets.

Gene Set Enrichment Analysis (GSEA) was used to search for GO and Reactome pathways, which revealed that the DNA replication, DNA integrity checkpoint, DNA repair, and signal transduction in response to

DNA damage were significantly enriched (Figure 13G and Supplementary Table 2). In addition, Reactome pathway analysis significantly enriched the cell cycle, cell cycle checkpoints, DNA repair, and neuronal system (Figure 13H). These results suggest that XRCC1 is associated with DNA repair-related pathways. Furthermore, we obtained the top 5 hub genes of 134 DEGs, including SOX4, PAX3, HOXD9, HOXC9, and GATA4 (Figure 13I). Moreover, the receiver operating characteristic (ROC) curve was carried out to analyze the effectiveness of hub gene expression in normal samples of GTEx-combined adjacent LGG tissues and LGG samples. XRCC1 (AUC=0.847), SOX4 (AUC=0.985), and HOXD9 (AUC=0.767) indicated that these three genes could be ideal biomarkers to distinguish LGG from non-tumor tissues (Figure 13K). The corresponding heat map data also showed that in LGG, XRCC1 was positively associated with the five genes mentioned above (Figure 13J).

Figure 11. The XRCC1 expression correlated with immune infiltration. (**A**) The expression of XRCC1 was strongly associated with the infiltration levels of various immune cells in the TIMER dataset. (**B**) Based on the XCELL database, we explored the significant correlation between the expression of XRCC1 and the infiltration levels of various immune cells. (*p < 0.05, **p < 0.01, and ***p < 0.001).

Table 1. Correlation analysis between XRCC1 and markers of immune cells in TIMER.

Cell type	Gene marker	None		Purity	
		Cor	P	Cor	P
B cell	CD19	0.151	***	0.156	***
	CD20(KRT20)	0.007	0.88	0.016	0.72
	CD38	0.117	**	0.101	*
CD8+ T cell	CD8A	-0.051	0.25	-0.07	0.13
	CD8B	-0.101	*	-0.106	*
Tfh	BCL6	0.175	***	0.179	***
	ICOS	0.07	0.11	0.06	0.19
	CXCR5	0.131	**	0.153	***
Th1	T-bet (TBX21)	0.108	*	0.112	*
	STAT4	-0.241	***	-0.245	***
	IL12RB2	-0.079	0.07	-0.093	*
	WSX1(IL27RA)	-0.023	0.60	-0.018	0.69
	STAT1	0.154	***	0.141	**
	IFN-γ (IFNG)	0.051	0.24	0.064	0.16
	TNF-α(TNF)	0.081	0.07	0.067	0.14
Th2	GATA3	0.179	***	0.181	***
	CCR3	0.099	*	0.098	*
	STAT6	0.082	0.06	0.081	0.08
	STAT5A	0.312	***	0.333	***
Th9	TGFBR2	0.136	**	0.141	**
	IRF4	0.055	0.21	0.089	0.05
	PU.1(SPI1)	0.292	***	0.302	***
Th17	STAT3	0.275	***	0.268	***
	IL-21R	-0.123	**	-0.131	**
	IL-23R	0.004	0.94	-0.017	0.72
Th22	IL-17A	-0.01	0.82	0.005	0.91
	CCR10	0.122	**	0.139	**
	AHR	0.104	*	0.087	0.06
Treg	FOXP3	-0.039	0.38	-0.024	0.60
	CD25(IL2RA)	-0.041	0.35	-0.01	0.83
	CCR8	0.033	0.46	0.038	0.41
T cell exhaustion	PD-1 (PDCD1)	0.112	*	0.11	*
	CTLA4	0.018	0.68	0.017	0.71
	LAG3	0.176	***	0.189	***
	TIM-3 (HAVCR2)	0.25	***	0.257	***
Macrophage	CD68	0.245	***	0.25	***
	CD11b (ITGAM)	0.252	***	0.265	***
M1	INOS (NOS2)	0.072	0.10	0.082	0.07
	IRF5	0.276	***	0.288	***
	COX2(PTGS2)	-0.044	0.32	-0.043	0.35
M2	CD163	0.088	*	0.089	0.05
	ARG1	-0.018	0.69	-0.019	0.67
	MRC1	-0.047	0.29	-0.03	0.52
	MS4A4A	0.16	***	0.174	***
TAM	CCL2	0.073	0.10	0.062	0.17
	CD80	0.165	***	0.161	***
	CD86	0.221	***	0.228	***

	CCR5	0.236	***	0.232	***
	CD14	0.211	***	0.203	***
Monocyte	CD16(FCGR3B)	-0.001	9.74-01	0.002	0.97
	CD115 (CSF1R)	0.238	***	0.25	***
	CD66b (CEACAM8)	0.06	0.17	0.054	0.24
Neutrophil	CD15(FUT4)	0.313	***	0.313	***
	CD11b (ITGAM)	0.252	***	0.265	***
Natural killer cell	XCL1	-0.012	0.78	0.003	0.94
	CD7	0.192	***	0.206	***
	KIR3DL1	-0.115	**	-0.116	*
Dendritic cell	CD1C(BDCA-1)	0.042	0.35	0.054	0.24
	CD141(THBD)	-0.005	0.91	0.006	0.90
	CD11c (ITGAX)	0.279	***	0.285	***

Tfh Follicular helper T cell, Th T helper cell, Treg Regulatory T cell, TAM Tumor-associated macrophage. None, correlation without adjustment. Purity, correlation adjusted by purity. Cor, R-value of Spearman's correlation. *P < 0.05; **P < 0.01; ***P < 0.001.
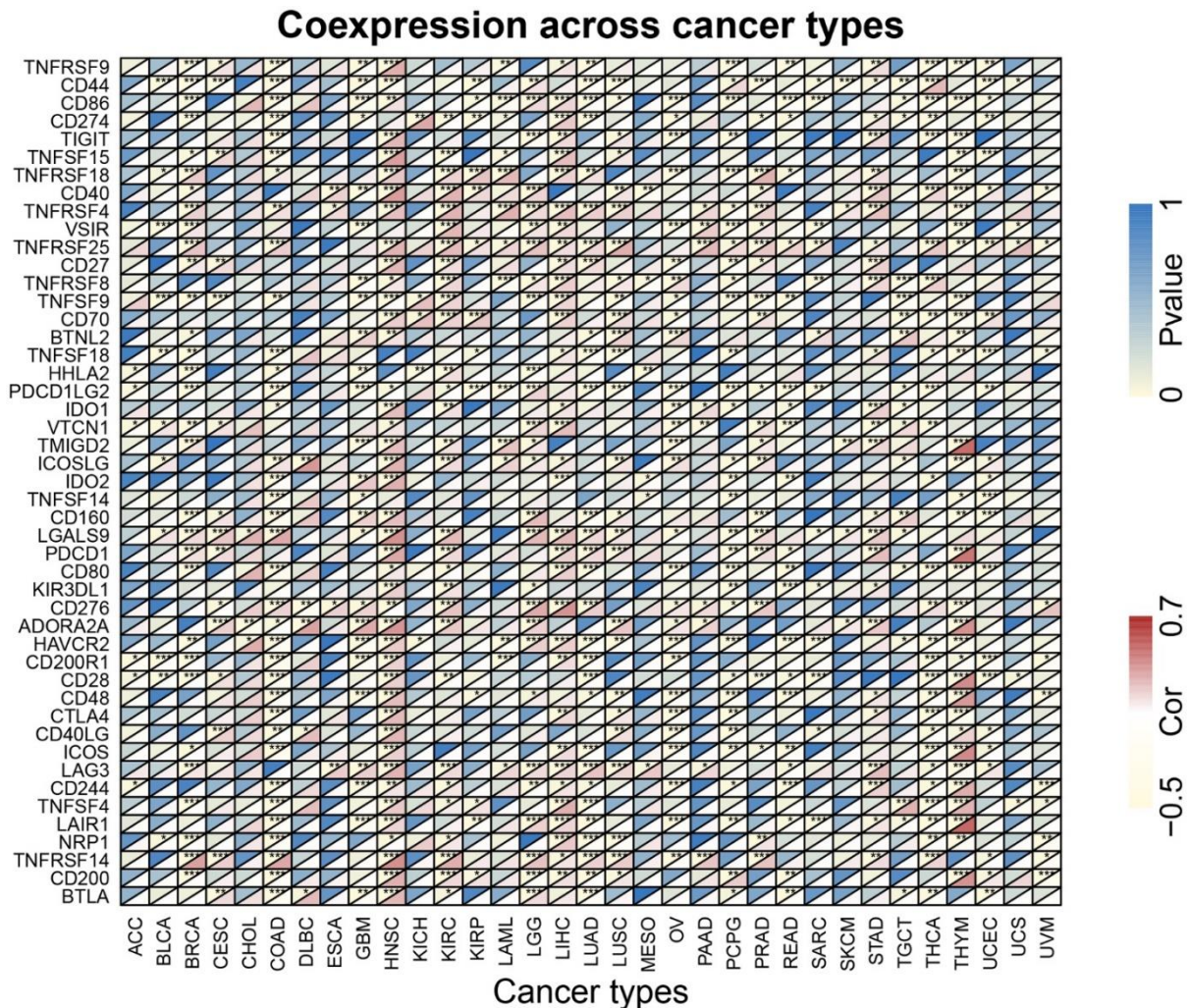
Figure 12. The association heatmaps between XRCC1 expression and immune checkpoint genes in pan-cancer. *P < 0.05, **P < 0.01, ***P < 0.001.

Table 2. Correlation between XRCC1 expression and clinicopathological characteristics in LGG.

Characteristic	Low expression of XRCC1	High expression of XRCC1	p
n	264	264	
WHO grade, n (%)			< 0.001
G2	133 (28.5%)	91 (19.5%)	
G3	104 (22.3%)	139 (29.8%)	
IDH status, n (%)			< 0.001
WT	25 (4.8%)	72 (13.7%)	
Mut	238 (45.3%)	190 (36.2%)	
1p/19q codeletion, n (%)			< 0.001
codel	132 (25%)	39 (7.4%)	
non-codel	132 (25%)	225 (42.6%)	
Primary therapy outcome, n (%)			0.073
PD	42 (9.2%)	68 (14.8%)	
SD	76 (16.6%)	70 (15.3%)	
PR	34 (7.4%)	30 (6.6%)	
CR	73 (15.9%)	65 (14.2%)	
Gender, n (%)			0.727
Female	122 (23.1%)	117 (22.2%)	
Male	142 (26.9%)	147 (27.8%)	
Race, n (%)			0.866
Asian	3 (0.6%)	5 (1%)	
Black or African American	11 (2.1%)	11 (2.1%)	
White	242 (46.8%)	245 (47.4%)	
Age, n (%)			0.139
<=40	141 (26.7%)	123 (23.3%)	
>40	123 (23.3%)	141 (26.7%)	
Histological type, n (%)			< 0.001
Astrocytoma	67 (12.7%)	128 (24.2%)	
Oligoastrocytoma	61 (11.6%)	73 (13.8%)	
Oligodendroglioma	136 (25.8%)	63 (11.9%)	
Laterality, n (%)			0.739
Left	126 (24.1%)	130 (24.9%)	
Midline	4 (0.8%)	2 (0.4%)	
Right	131 (25%)	130 (24.9%)	
Age, median (IQR)	40 (32.75, 51)	41.5 (31, 55)	0.484

Abbreviations: CR, complete response; PD, progressive disease; SD, stable disease; PR, partial response.

Analysis of genetic mutation and methylation levels of XRCC1 and hub-gene and pathway regulation in LGG

We performed co-analysis of XRCC1 with its correlated genes, namely GATA4, HOXC9, HOXD9, PAX3, and SOX4. The CNV states of these genes in LGG were investigated, as depicted in Figure 14A. XRCC1 exhibited a high susceptibility to mutation, primarily heterozygous deletion, while GATA4 showed heterozygous amplification as the main CNV type. The CNV analysis in Figure 14B confirmed the vulnerability

of these genes to heterozygous deletions, with XRCC1 being the most mutation prone. Figure 14C demonstrated a significant correlation between CNV and XRCC1 expression levels in LGG, while a weak correlation was observed for SOX4 and PAX3. Survival analysis based on hypermethylation and hypomethylation patterns (Figure 14D) revealed that hypermethylation of HOXD9 was associated with a higher survival risk in LGG, whereas hypermethylation of XRCC1 and PAX3 indicated a lower survival risk. Furthermore, in Figure 14E, the expression levels of XRCC1 and its correlated genes
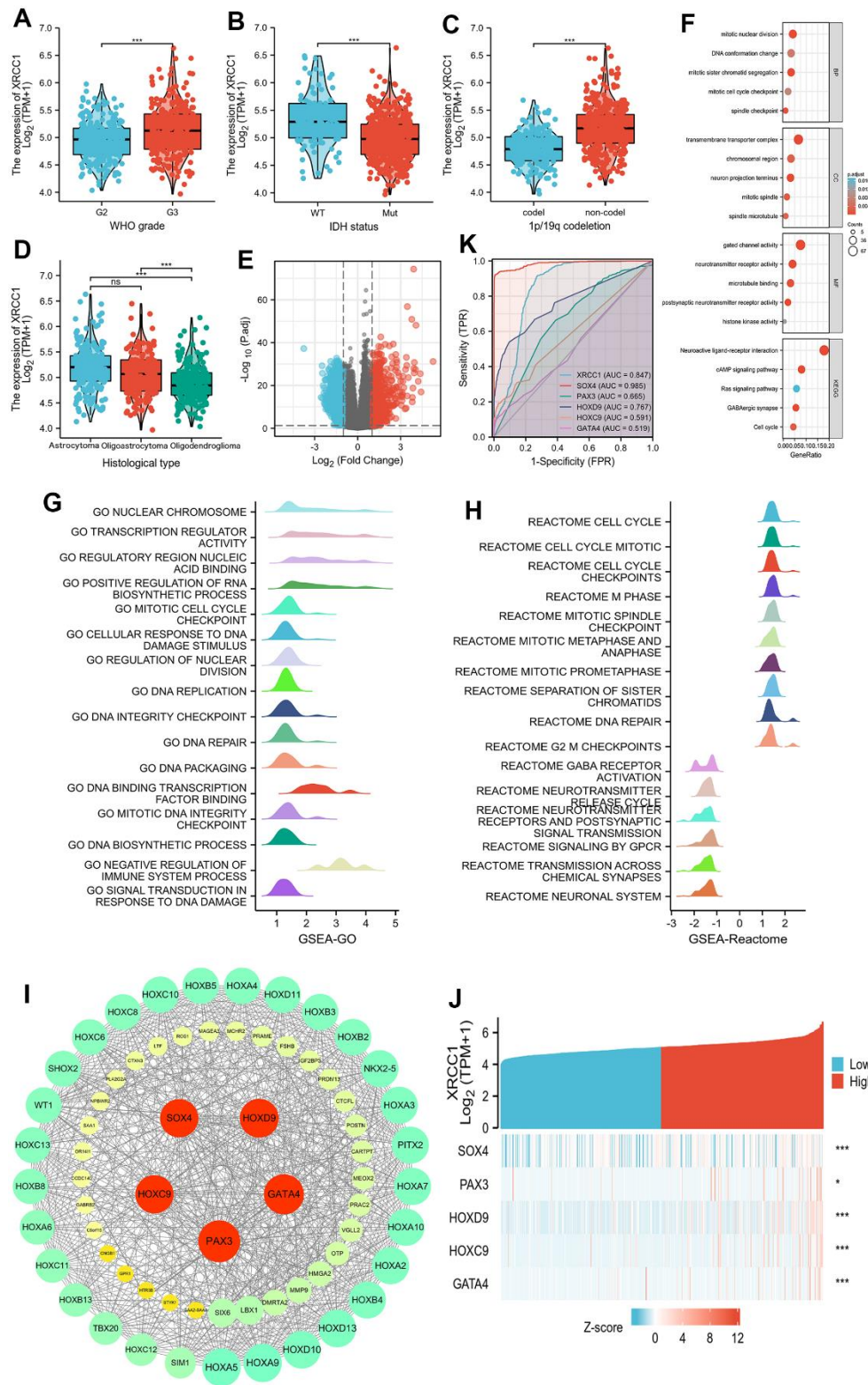
Figure 13. Associations between XRCC1 expression and different clinical characteristics in LGG. PPI network building and GO, KEGG, and GSEA analyses between XRCC1 high and low expression groups in LGG. Hub genes positively correlated with XRCC1 expression in LGG and hub genes' receiver operating characteristic (ROC) curve. (**A**) WHO grade. (**B**) IDH status. (**C**) 1p/19q codeletion. (**D**) Histological type (ns, p≥0.05, *p<0.05, **p<0.01, ***p<0.001). (**E**) volcano plot of DEGs (red: upregulation, blue: downregulation). (**F**) GO and KEGG analyses of DEGs. (**G**, **H**) significant GSEA results for DEGs, including GO terms and Reactome pathways. (**I**) PPI network. (**J**) the gene coexpression heatmap of the hub genes. (**K**) ROC curve of hub genes.

Table 3. XRCC1 expression associated with clinicopathologic characteristics (Logistic Regression).

Characteristics	Total (N)	Odds ratio (OR)	P-value
WHO grade (G3 vs. G2)	467	1.953 (1.354-2.829)	<0.001
IDH status (Mut vs. WT)	525	0.277 (0.167-0.448)	<0.001
1p/19q codeletion (non-codel vs. codel)	528	5.769 (3.834-8.840)	<0.001
Primary therapy outcome (PR&CR vs. PD&SD)	458	0.759 (0.524-1.098)	0.144
Gender (Male vs. Female)	528	1.079 (0.766-1.521)	0.662
Race (White vs. Asian&Black or African American)	517	0.886 (0.418-1.858)	0.748
Age (>40 vs. <=40)	528	1.314 (0.934-1.852)	0.117
Histological type (Oligoastrocytoma&Oligodendroglioma vs. Astrocytoma)	528	0.361 (0.249-0.520)	<0.001
Laterality (Right vs. Left&Midline)	523	0.977 (0.693-1.377)	0.896

exhibited negative correlation with methylation levels. Notably, XRCC1 and PAX3 showed substantial statistical significance, suggesting their deregulation. Figure 14F illustrated the influence of these six genes on ten LGG-related pathways. Increased expression of XRCC1 in LGG activated the Cell cycle, DNA damage response, and Hormone AR pathways, while inhibiting Apoptosis, EMT, RAS/MAPK, RTK, and TSC/mTOR pathways. The DNA damage response and EMT pathways were predominantly activated, whereas the RAS/MAPK and RTK pathways were primarily inhibited. Both Apoptosis and PI3K/AKT pathways showed elements of activation and/or inhibition. Moreover, Figure 14H demonstrated the correlation between XRCC1 and its correlated genes' expression levels and drug sensitivity in LGG for specific drugs. Notably, XRCC1 expression was negatively correlated with drug sensitivity in LGG, potentially explaining its classification as a pro-cancer gene. Conversely, HOXC9 expression exhibited a positive correlation with drug sensitivity in LGG. SOX4, PAX3, and HOXD9 displayed limited relevance to drugs.

DISCUSSION

DNA repair is critical in protecting the cellular genome from damage caused by carcinogens or ionizing radiation [47]. XRCC1 is required for DNA single-strand break repair in human cells. The reduced DNA single-strand break repair and genomic instability caused by XRCC1 defects may contribute to cancer development [48]. A large number of studies have reported that XRCC1 is associated with the development, progression, and prognosis of a variety of cancers, such as thyroid cancer, gastric cancer, non-small cell lung cancer, and cervical cancer. Moreover,

XRCC1 Arg194Trp and XRCC1 Arg399Gln were revealed to be strongly associated with susceptibility to glioma among the Chinese population according to a large case-control study [49]. Still, the exact mechanism is unclear [47, 48, 50–55]. Therefore, we systematically analyzed XRCC1 concerning expression, prognostic types, immune invasion, methylation, phosphorylation, and molecular typing in various cancers.

High XRCC1 gene expression was associated with poor OS in LAML and LGG and poor DFS in LGG, LIHC, and LUAD. That is, increased expression of XRCC1 corresponds to a poor prognosis in most cancers. XRCC1, a gene closely related to DNA damage repair, plays an important role in tumor resistance to radiotherapy and chemotherapy. Radiotherapy has been reported to be more effective in patients with non-small cell lung cancer who have XRCC1 gene mutations [56]. This phenomenon also exists in breast, head, neck and rectal cancer [57–59]. In addition, chemotherapy's effect and toxicity were greater in patients with XRCC1 mutated non-small cell lung and gastric cancers than in those with high XRCC1 expression [60–62]. All this evidence suggests that XRCC1 is closely associated with tumor resistance. The main mechanism of action of chemotherapy and radiotherapy is to damage the DNA of tumor cells, and the effectiveness depends on the ability to damage the DNA [63, 64]. Thus, DNA repair interferes with chemotherapy and radiotherapy. For example, glycogen synthase kinase-3β, DNA-dependent protein kinase, and poly (ADP-ribose) polymerase family with DNA repair capabilities reduce the sensitivity of tumors to chemotherapy and radiotherapy [65–67]. At the same time, the enzyme complex formed by XRCC1 is optimized for single-strand break repair and also participates in other repair pathways, playing an important role in DNA repair [68, 69]. Therefore, it
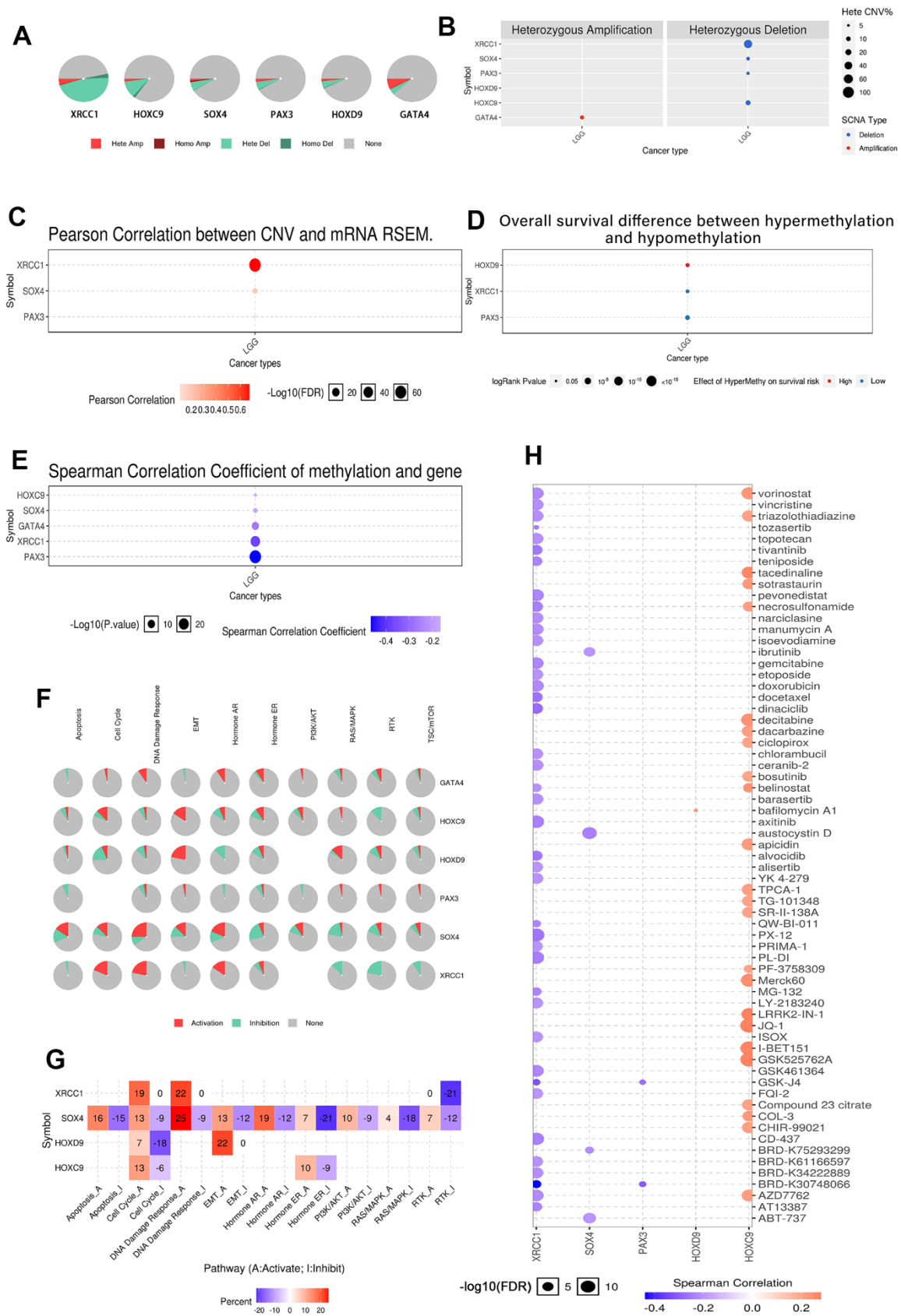
Figure 14. Analysis of genetic mutation and methylation levels of XRCC1 and hub-gene and pathway regulation in LGG. (A) Homozygous/heterozygous CNV of XRCC1 and its related genes in LGG. Homo Amp: homozygous amplification; Hete Amp: heterozygous

amplification; Homo Del: homozygous deletion; Hete Del: heterozygous deletion; None: without CNV. (**B**) The heterozygous CNV of XRCC1 and (**C**) the correlation between CNV and mRNA RSEM. The heterozygous CNV of XRCC1 and the correlation between CNV and mRNA RSEM in LGG were plotted to utilize GSCALite. (**D**) The overall survival discrepancy between hypermethylation and hypomethylation of XRCC1 and its related genes in LGG. (**E**) In the correlation between methylation and gene expression in LGG, blue represented a negative correlation, while red represented a positive correlation. (**F**) XRCC1 and hub genes influence pathways that participate in the development, growth, and progression of LGG. (**G**) The inferred activity of the identified four target genes in pathways that participate in the development, growth, and progression of LGG. A and I to mark the active and inhibited pathways, respectively. (**H**) The correlation of XRCC1 expression and LGG drug sensitivity.

is likely that XRCC1 contributes to the poor prognosis of tumor patients by promoting DNA repair and reducing the sensitivity of tumors to chemotherapy and radiotherapy.

DNA methylation and histone modifications such as methylation and phosphorylation are common epigenetic modifications that play an important role in the transcriptional regulation of genes involved in cell cycle progression, proliferation, apoptosis and cell death [70]. Alterations in the epigenetically controlled expression of these genes may also mediate oncogenic processes [71]. It has been demonstrated that XRCC1 phosphorylation by CK2 is required for its stability and efficient DNA repair and that CK2 phosphorylation of XRCC1 facilitates dissociation from DNA and single-strand break formation during BER [72]. In the present study, we found that the T453 site of XRCC1 protein exhibited higher phosphorylation levels in the breast, colon, LUAD, UCEC, and PAAD and that the expression status of XRCC1 phosphorylated proteins (S241, S266, S268, S447, S461 S475, and T453 sites) in certain tumor tissues and normal tissues was somewhat of a difference. This suggests that XRCC1 is also associated with phosphorylation in the development of various types of cancer. In addition, we found a mutation rate of XRCC1 of 1.8% in all tumor patients and a copy number deletion of XRCC1 in all DLBC cases. This suggests that mutations in XRCC1 are associated with cancer development and progression.

Another important finding of this study is that XRCC1-associated infiltration of various immune cells correlates with cancer prognosis. Prognostic analysis showed that high XRCC1 gene expression was associated with poor OS and DFS in LGG. The immune cell infiltration results demonstrated that T cell CD4+ was positively correlated with XRCC1 in LGG. It is well known that T cell CD4+ epitopes are important targets of immunity against infectious diseases and cancer [73]. Several studies have shown that T cell CD4+ is associated with poor prognosis of tumors [74–76], which coincides with the results of our research. Therefore, the high expression of XRCC1 leads to poor prognosis in LGG and is likely to be associated with T cell CD4+ infiltration.

On the other hand, XRCC1 was negatively correlated with B cells (p<0.001). Numerous studies have shown that B cell has a beneficial effect on cancer prognosis [77–80], which supports our view from another perspective. Overall, XRCC1-mediated infiltration of various immune cells in the tumor microenvironment is likely to be closely associated with tumor prognosis. In addition, XRCC1 was significantly associated with most immunosuppressive and immunostimulatory genes in BRCA, COAD, HNSC, LIHC, and THYM. Immune checkpoints are regulators of the immune system that are essential for self-tolerance and prevent the immune system from attacking cells indiscriminately. However, some cancers can protect themselves from attack by tricking immune checkpoints [81]. And the present study found that XRCC1 was significantly correlated with most immunosuppressive and immunostimulatory genes in some tumors, suggesting that the immune escape mechanism of tumors may be associated with XRCC1. TMB is a genetic signature of tumor tissue, defined as the number of non-genetic mutations per million bases in the studied genomic sequence, and its measurement has been achieved by second-generation sequencing [82]. TMB has shown potential as a predictive biomarker with multiple applications, including the association between different reported TMB levels and patient response to immune checkpoint inhibitor therapy in various cancers [83]. The gene expression level of XRCC1 was strongly associated with TMB status across multiple cancer types, which on the other hand, supports the previous conclusions about XRCC1 and immune checkpoints. Taken together, the above results strongly suggest the potential of XRCC1 as an anti-cancer immunotherapy target.

LGGs are a heterogeneous group of tumors that include predominantly glial histology, including astrocytes and/or oligodendrocytes, and tumors with mixed neuron-glial cell morphology. These tumors are considered Grade I and Grade II according to the current WHO classification [84]. Since XRCC1 expression correlates with the prognosis of each type of LGG, we further explored the clinical features, gene function enrichment, mutations, methylation, and drug resistance aspects of XRCC1 in LGG. Based on our analysis of clinical features and gene expression data of 529 primary LGG cases, we found that

XRCC1 expression was not only correlated with WHO pathological classification but also negatively correlated with drug sensitivity in LGG, which may also explain why high XRCC1 expression implies poor prognosis in LGG. In addition, we identified XRCC1 (AUC=0.847), SOX4 (AUC=0.985), and HOXD9 (AUC=0.767) as three molecules that could be ideal biomarkers to distinguish LGG from non-tumor tissues. Furthermore, DNA integrity checkpoint, DNA repair, and signal transduction in response to DNA damage were significantly enriched, and these results suggest that XRCC1 pathways are associated with DNA repair in LGG. These results indicate that XRCC1 and DNA repair-related pathways may play a role in the development of LGG.

Our first pan-cancer analysis of XRCC1 revealed a statistical correlation between XRCC1 expression and clinical prognosis, DNA methylation, protein phosphorylation, TMB, MSI, immune cell infiltration, and immune checkpoints. Our results suggest that XRCC1 can be an independent prognostic and diagnostic factor for many tumors. Its expression levels lead to different prognostic outcomes and tumour diagnostic results. However, despite our comprehensive and systematic analysis of XRCC1 and the use of different public databases for cross-validation, this study still has some limitations. First, the gene microarray and sequencing data from different databases exhibited differences and lacked granularity and specificity, which may cause systematic bias. Future studies should rely on higher resolution methods, such as single-cell RNA sequencing, to overcome this problem. Second, *in vivo/in vitro* experiments are needed to demonstrate our results regarding the potential function of XRCC1 in LGG, which may increase the credibility of our results. Third, we could not demonstrate that XRCC1 expression affects patient survival through immune infiltration, even though we found that XRCC1 expression was associated with immune cell infiltration in tumors and patient survival. Therefore, further prospective studies are needed to explore the relationship between XRCC1 expression and immune infiltration in cancer patient populations.

CONCLUSIONS

We conducted a comprehensive investigation into the potential of XRCC1 as a valuable diagnostic and prognostic indicator in diverse cancer types. The positive correlation between XRCC1 expression and immune cell infiltration suggests its involvement in the tumor immune microenvironment. Moreover, the heterogeneity of XRCC1 is highlighted by its differential expression across immunological and molecular subtypes of different malignancies. In certain tumors, XRCC1 may play a role in modulating the tumor immune landscape by regulating the expression of immune checkpoint genes. Overall, XRCC1 emerges as a promising biomarker for cancer diagnosis, prognosis, and immunological assessment, particularly in the context of LGG. This study employs a systems biology approach to analyze the molecular mechanisms behind the development of cancer in an effort to improve our knowledge of cancer biology and yield novel insights for therapeutic approaches. Future investigations ought to concentrate on unraveling the mechanism underlying XRCC1's involvement in various cancer types, particularly in immuno-modulation. By closely examining the relationship between XRCC1 and immune cell infiltration, we will seek to elucidate the precise mechanism underlying XRCC1 in regulating tumor immune response. Furthermore, exploring XRCC1's potential role in tumor immunotherapy and assessing its viability as a therapeutic target will provide valuable insights for the design of tailored cancer therapies and immunotherapy approaches.

Abbreviations

ACC: Adrenocortical carcinoma; AML: Acute myeloid leukemia; BER: Base excision repair; BLCA: Bladder urothelial carcinoma; BRCA: Breast invasive carcinoma; c-BioPortal: cBio Cancer Genomics Portal; CCLE: Cancer Cell Line Encyclopedia; CHOL: Cholangiocarcinoma; CESC: Cervical squamous cell carcinoma and endocervical adenocarcinoma; CK2: Casein kinase 2; CNV: Copy number variation; COAD: Colon adenocarcinoma; DEGs: Differential expression genes; DFS: Disease-free survival; DSS: Disease-specific survival; ESCA: Esophageal carcinoma; FC: Fold-change; GDC: Genomic Data Commons; GBM: Glioblastoma multiforme; GSEA: Gene Set Enrichment Analysis; GTEx: Genotype Tissue Expression; HNSC: Head and neck adenocarcinoma; HPA: Human Protein Atlas; KICH: Kidney chromophobe; KIRC: Kidney renal clear cell carcinoma; KIRP: Kidney renal papillary cell carcinoma; LGG: Lower grade glioma; Lig-III: Ligase IIIα; LIHC: Liver hepatocellular carcinoma; LUSC: Lung squamous cell carcinoma; LUAD: Lung adenocarcinoma; MESO: Mesothelioma; MMEJ: Microhomology-mediated end joining; MSI: Microsatellite instability; OS: Overall survival; OSCC: Oral squamous cell carcinoma; PFS: Progression-free survival; READ: Rectum adenocarcinoma; ROC: Receiver operating characteristic; SARC: Sarcoma; SKCM: Skin cutaneous melanoma; SSBR: Single-strand break repair; STAD: Stomach adenocarcinoma; STRING: Search Tool for the Retrieval of Interacting

Genes/Proteins; TAM: Tumor-associated macrophages; TGCT: Testicular germ cell tumor; THYM: Thymoma; TMB: Tumor Mutation Burden; TME: Tumor microenvironment; TPM: Transcripts per million reads; PCPG: Pheochromocytoma and paraganglioma; PD-L1: Programmed death ligand 1; PD-1: Programmed cell death 1; PPI: Protein-Protein Interaction; PRAD: Prostate adenocarcinoma; UCS: Uterine carcinosarcoma; XRCC1: X-ray repair cross-complementation group 1.

AUTHOR CONTRIBUTIONS

HC and GT conceived the study. GW, HC, YL, RP, CJ and YS drafted the manuscript and performed the analysis. XY, CJ, and YS performed the literature search and collected the data. PL and LH contributed to drafting the manuscript and interpreting the data. GY, HC and GT revised the manuscript. All authors reviewed and approved the final manuscript.

ACKNOWLEDGMENTS

CONFLICTS OF INTEREST

FUNDING

REFERENCES

1. Bray F, Laversanne M, Weiderpass E, Soerjomataram I. The ever-increasing importance of cancer as a leading cause of premature death worldwide. Cancer. 2021; 127:3029–30.
   https://doi.org/10.1002/cncr.33587 PMID:34086348

2. de Sá VK, Coelho JC, Capelozzi VL, de Azevedo SJ. Lung cancer in Brazil: epidemiology and treatment challenges. Lung Cancer (Auckl). 2016; 7:141–8.
   https://doi.org/10.2147/LCTT.S93604
   PMID:28210170

3. Dodgshun AJ, Fukuoka K, Edwards M, Bianchi VJ, Das A, Sexton-Oates A, Larouche V, Vanan MI, Lindhorst S, Yalon M, Mason G, Crooks B, Constantini S, et al. Germline-driven replication repair-deficient high-grade gliomas exhibit unique hypomethylation patterns. Acta Neuropathol. 2020; 140:765–76.
   https://doi.org/10.1007/s00401-020-02209-8
   PMID:32895736

4. Elias-Rizk T, El Hajj J, Segal-Bendirdjian E, Hilal G. The long non coding RNA H19 as a biomarker for breast cancer diagnosis in Lebanese women. Sci Rep. 2020; 10:22228.
   https://doi.org/10.1038/s41598-020-79285-z
   PMID:33335214

5. Jayaraj R, Raymond G, Krishnan S, Tzou KS, Baxi S, Ram MR, Govind SK, Chandramoorthy HC, Abu-Khzam FN, Shaw P. Clinical Theragnostic Potential of Diverse miRNA Expressions in Prostate Cancer: A Systematic Review and Meta-Analysis. Cancers (Basel). 2020; 12:1199.
   https://doi.org/10.3390/cancers12051199
   PMID:32397507

6. Kast RE, Michael AP, Sardi I, Burns TC, Heiland T, Karpel-Massler G, Kamar FG, Halatsch ME. A New Treatment Opportunity for DIPG and Diffuse Midline Gliomas: 5-ALA Augmented Irradiation, the 5aai Regimen. Brain Sci. 2020; 10:51.
   https://doi.org/10.3390/brainsci10010051
   PMID:31963414

7. Siegel R, Naishadham D, Jemal A. Cancer statistics, 2012. CA Cancer J Clin. 2012; 62:10–29.
   https://doi.org/10.3322/caac.20138
   PMID:22237781

8. Bahmad HF, Chalhoub RM, Harati H, Bou-Gharios J, Assi S, Ballout F, Monzer A, Msheik H, Araji T, Elajami MK, Ghanem P, Chamaa F, Kadara H, et al. Tideglusib attenuates growth of neuroblastoma cancer stem/progenitor cells *in vitro* and *in vivo* by specifically targeting GSK-3β. Pharmacol Rep. 2021; 73:211–26.
   https://doi.org/10.1007/s43440-020-00162-7
   PMID:33030673

9. Smith RA, Andrews KS, Brooks D, Fedewa SA, Manassaram-Baptiste D, Saslow D, Wender RC. Cancer screening in the United States, 2019: A review of current American Cancer Society guidelines and current issues in cancer screening. CA Cancer J Clin. 2019; 69:184–210.
   https://doi.org/10.3322/caac.21557
   PMID:30875085

10. Zheng G, Chen X, Xu B, Zhang J, Lv X, Li J, Li F, Hu S, Zhang T, Li Y. Plasticity of language pathways in patients with low-grade glioma: A diffusion tensor imaging study. Neural Regen Res. 2013; 8:647–54.
https://doi.org/10.3969/j.issn.1673-5374.2013.07.009
PMID:25206710

11. Zhao S, Ji W, Shen Y, Fan Y, Huang H, Huang J, Lai G, Yuan K, Cheng C. Expression of hub genes of endothelial cells in glioblastoma-A prognostic model for GBM patients integrating single-cell RNA sequencing and bulk RNA sequencing. BMC Cancer. 2022; 22:1274.
https://doi.org/10.1186/s12885-022-10305-z
PMID:36474171

12. Zhao S, Chi H, Ji W, He Q, Lai G, Peng G, Zhao X, Cheng C. A Bioinformatics-Based Analysis of an Anoikis-Related Gene Signature Predicts the Prognosis of Patients with Low-Grade Gliomas. Brain Sci. 2022; 12:1349.
https://doi.org/10.3390/brainsci12101349
PMID:36291283

13. Haddad AF, Young JS, Oh JY, Okada H, Aghi MK. The immunology of low-grade gliomas. Neurosurg Focus. 2022; 52:E2.
https://doi.org/10.3171/2021.11.FOCUS21587
PMID:35104791

14. Gabel N, Altshuler DB, Brezzell A, Briceño EM, Boileau NR, Miklja Z, Kluin K, Ferguson T, McMurray K, Wang L, Smith SR, Carlozzi NE, Hervey-Jumper SL. Health Related Quality of Life in Adult Low and High-Grade Glioma Patients Using the National Institutes of Health Patient Reported Outcomes Measurement Information System (PROMIS) and Neuro-QOL Assessments. Front Neurol. 2019; 10:212.
https://doi.org/10.3389/fneur.2019.00212
PMID:30930834

15. Chi H, Xie X, Yan Y, Peng G, Strohmer DF, Lai G, Zhao S, Xia Z, Tian G. Natural killer cell-related prognosis signature characterizes immune landscape and predicts prognosis of HNSCC. Front Immunol. 2022; 13:1018685.
https://doi.org/10.3389/fimmu.2022.1018685
PMID:36263048

16. Bednar F, Pasca di Magliano M. Chemotherapy and Tumor Evolution Shape Pancreatic Cancer Recurrence after Resection. Cancer Discov. 2020; 10:762–4.
https://doi.org/10.1158/2159-8290.CD-20-0359
PMID:32482663

17. Wyld L, Audisio RA, Poston GJ. The evolution of cancer surgery and future perspectives. Nat Rev Clin Oncol. 2015; 12:115–24.
https://doi.org/10.1038/nrclinonc.2014.191
PMID:25384943

18. Topper MJ, Vaz M, Marrone KA, Brahmer JR, Baylin SB. The emerging role of epigenetic therapeutics in immuno-oncology. Nat Rev Clin Oncol. 2020; 17:75–90.
https://doi.org/10.1038/s41571-019-0266-5
PMID:31548600

19. Chi H, Peng G, Wang R, Yang F, Xie X, Zhang J, Xu K, Gu T, Yang X, Tian G. Cuprotosis Programmed-Cell-Death-Related lncRNA Signature Predicts Prognosis and Immune Landscape in PAAD Patients. Cells. 2022; 11:3436.
https://doi.org/10.3390/cells11213436
PMID:36359832

20. Kobayashi Y, Lim SO, Yamaguchi H. Oncogenic signaling pathways associated with immune evasion and resistance to immune checkpoint inhibitors in cancer. Semin Cancer Biol. 2020; 65:51–64.
https://doi.org/10.1016/j.semcancer.2019.11.011
PMID:31874279

21. Hiller JG, Perry NJ, Poulogiannis G, Riedel B, Sloan EK. Perioperative events influence cancer recurrence risk after surgery. Nat Rev Clin Oncol. 2018; 15:205–18.
https://doi.org/10.1038/nrclinonc.2017.194
PMID:29283170

22. Bankoglu EE, Schuele C, Stopper H. Cell survival after DNA damage in the comet assay. Arch Toxicol. 2021; 95:3803–13.
https://doi.org/10.1007/s00204-021-03164-3
PMID:34609522

23. Dianov GL, Parsons JL. Co-ordination of DNA single strand break repair. DNA Repair (Amst). 2007; 6:454–60.
https://doi.org/10.1016/j.dnarep.2006.10.009
PMID:17123872

24. London RE. XRCC1 - Strategies for coordinating and assembling a versatile DNA damage response. DNA Repair (Amst). 2020; 93:102917.
https://doi.org/10.1016/j.dnarep.2020.102917
PMID:33087283

25. Carter RJ, Parsons JL. Base Excision Repair, a Pathway Regulated by Posttranslational Modifications. Mol Cell Biol. 2016; 36:1426–37.
https://doi.org/10.1128/MCB.00030-16
PMID:26976642

26. Mittal RD, Mandal RK, Gangwar R. Base excision repair pathway genes polymorphism in prostate and bladder cancer risk in North Indian population. Mech Ageing Dev. 2012; 133:127–32.
https://doi.org/10.1016/j.mad.2011.10.002
PMID:22019847

27. Fagerberg L, Hallström BM, Oksvold P, Kampf C, Djureinovic D, Odeberg J, Habuka M, Tahmasebpoor S, Danielsson A, Edlund K, Asplund A, Sjöstedt E,

Lundberg E, et al. Analysis of the human tissue-specific expression by genome-wide integration of transcriptomics and antibody-based proteomics. Mol Cell Proteomics. 2014; 13:397–406.
https://doi.org/10.1074/mcp.M113.035600
PMID:24309898

28. Mian M, McNamara MG, Doherty M, Hedley D, Knox JJ, Serra S. Predictive and prognostic values of ERCC1 and XRCC1 in biliary tract cancers. J Clin Pathol. 2016; 69:695–701.
https://doi.org/10.1136/jclinpath-2015-203397
PMID:26763622

29. Mei PJ, Bai J, Miao FA, Li ZL, Chen C, Zheng JN, Fan YC. Relationship between expression of XRCC1 and tumor proliferation, migration, invasion, and angiogenesis in glioma. Invest New Drugs. 2019; 37:646–57.
https://doi.org/10.1007/s10637-018-0667-9
PMID:30328556

30. Metin Mahmutoglu A, Gunes S, Asci R, Henkel R, Aydin O. Association of XRCC1 and ERCC2 promoters' methylation with chromatin condensation and sperm DNA fragmentation in idiopathic oligoasthenoteratozoospermic men. Andrologia. 2021; 53:e13925.
https://doi.org/10.1111/and.13925
PMID:33355950

31. Nissar B, Kadla SA, Wani KA, Shah IA, Ganai BA. Promoter CpG island hypermethylation and down regulation of XRCC1 gene can augment in the gastric carcinogenesis events. Mol Biol Rep. 2021; 48:405–12.
https://doi.org/10.1007/s11033-020-06064-4
PMID:33394233

32. de Sousa MML, Bjørås KØ, Hanssen-Bauer A, Solvang-Garten K, Otterlei M. p38 MAPK signaling and phosphorylations in the BRCT1 domain regulate XRCC1 recruitment to sites of DNA damage. Sci Rep. 2017; 7:6322.
https://doi.org/10.1038/s41598-017-06770-3
PMID:28740101

33. Dutta A, Eckelmann B, Adhikari S, Ahmed KM, Sengupta S, Pandey A, Hegde PM, Tsai MS, Tainer JA, Weinfeld M, Hegde ML, Mitra S. Microhomology-mediated end joining is activated in irradiated human cells due to phosphorylation-dependent formation of the XRCC1 repair complex. Nucleic Acids Res. 2017; 45:2585–99.
https://doi.org/10.1093/nar/gkw1262
PMID:27994036

34. Vivian J, Rao AA, Nothaft FA, Ketchum C, Armstrong J, Novak A, Pfeil J, Narkizian J, Deran AD, Musselman-Brown A, Schmidt H, Amstutz P, Craft B, et al. Toil enables reproducible, open source, big biomedical data analyses. Nat Biotechnol. 2017; 35:314–6.
https://doi.org/10.1038/nbt.3772
PMID:28398314

35. Tang Z, Li C, Kang B, Gao G, Li C, Zhang Z. GEPIA: a web server for cancer and normal gene expression profiling and interactive analyses. Nucleic Acids Res. 2017; 45:W98–102.
https://doi.org/10.1093/nar/gkx247
PMID:28407145

36. Chandrashekar DS, Bashel B, Balasubramanya SAH, Creighton CJ, Ponce-Rodriguez I, Chakravarthi BV, Varambally S. UALCAN: A Portal for Facilitating Tumor Subgroup Gene Expression and Survival Analyses. Neoplasia. 2017; 19:649–58.
https://doi.org/10.1016/j.neo.2017.05.002
PMID:28732212

37. Chen F, Chandrashekar DS, Varambally S, Creighton CJ. Pan-cancer molecular subtypes revealed by mass-spectrometry-based proteomic characterization of more than 500 human cancers. Nat Commun. 2019; 10:5679.
https://doi.org/10.1038/s41467-019-13528-0
PMID:31831737

38. Gao J, Aksoy BA, Dogrusoz U, Dresdner G, Gross B, Sumer SO, Sun Y, Jacobsen A, Sinha R, Larsson E, Cerami E, Sander C, Schultz N. Integrative analysis of complex cancer genomics and clinical profiles using the cBioPortal. Sci Signal. 2013; 6:pl1.
https://doi.org/10.1126/scisignal.2004088
PMID:23550210

39. Ru B, Wong CN, Tong Y, Zhong JY, Zhong SSW, Wu WC, Chu KC, Wong CY, Lau CY, Chen I, Chan NW, Zhang J. TISIDB: an integrated repository portal for tumor-immune system interactions. Bioinformatics. 2019; 35:4200–2.
https://doi.org/10.1093/bioinformatics/btz210
PMID:30903160

40. Jensen MA, Ferretti V, Grossman RL, Staudt LM. The NCI Genomic Data Commons as an engine for precision medicine. Blood. 2017; 130:453–9.
https://doi.org/10.1182/blood-2017-03-735654
PMID:28600341

41. Li T, Fan J, Wang B, Traugh N, Chen Q, Liu JS, Li B, Liu XS. TIMER: A Web Server for Comprehensive Analysis of Tumor-Infiltrating Immune Cells. Cancer Res. 2017; 77:e108–10.
https://doi.org/10.1158/0008-5472.CAN-17-0307
PMID:29092952

42. Zhao ZJ, Wei DP, Zheng RZ, Peng T, Xiao X, Li FS. The Gene Coexpression Analysis Identifies Functional Modules Dynamically Changed After Traumatic Brain Injury. Comput Math Methods Med. 2021; 2021:5511598.

https://doi.org/10.1155/2021/5511598
PMID:33953790

43. Yu G, Wang LG, Han Y, He QY. clusterProfiler: an R package for comparing biological themes among gene clusters. OMICS. 2012; 16:284–7.
https://doi.org/10.1089/omi.2011.0118
PMID:22455463

44. Szklarczyk D, Franceschini A, Wyder S, Forslund K, Heller D, Huerta-Cepas J, Simonovic M, Roth A, Santos A, Tsafou KP, Kuhn M, Bork P, Jensen LJ, von Mering C. STRING v10: protein-protein interaction networks, integrated over the tree of life. Nucleic Acids Res. 2015; 43:D447–52.
https://doi.org/10.1093/nar/gku1003 PMID:25352553

45. Shannon P, Markiel A, Ozier O, Baliga NS, Wang JT, Ramage D, Amin N, Schwikowski B, Ideker T. Cytoscape: a software environment for integrated models of biomolecular interaction networks. Genome Res. 2003; 13:2498–504.
https://doi.org/10.1101/gr.1239303 PMID:14597658

46. Liu CJ, Hu FF, Xia MX, Han L, Zhang Q, Guo AY. GSCALite: a web server for gene set cancer analysis. Bioinformatics. 2018; 34:3771–2.
https://doi.org/10.1093/bioinformatics/bty411
PMID:29790900

47. Schneider J, Classen V, Helmig S. XRCC1 polymorphism and lung cancer risk. Expert Rev Mol Diagn. 2008; 8:761–80.
https://doi.org/10.1586/14737159.8.6.761
PMID:18999926

48. Brem R, Hall J. XRCC1 is required for DNA single-strand break repair in human cells. Nucleic Acids Res. 2005; 33:2512–20.
https://doi.org/10.1093/nar/gki543
PMID:15867196

49. Pan WR, Li G, Guan JH. Polymorphisms in DNA repair genes and susceptibility to glioma in a chinese population. Int J Mol Sci. 2013; 14:3314–24.
https://doi.org/10.3390/ijms14023314
PMID:23385236

50. Chen J, Zhao QW, Shi GM, Wang LR. XRCC1 Arg399Gln and clinical outcome of platinum-based treatment for advanced non-small cell lung cancer: a meta-analysis in 17 studies. J Zhejiang Univ Sci B. 2012; 13:875–83.
https://doi.org/10.1631/jzus.B1200083
PMID:23125080

51. Liu GC, Zhou YF, Su XC, Zhang J. Interaction between TP53 and XRCC1 increases susceptibility to cervical cancer development: a case control study. BMC Cancer. 2019; 19:24.
https://doi.org/10.1186/s12885-018-5149-0
PMID:30616520

52. Cao Z, Song J, Wang J, Guo X, Yu S, Dong W. Association between polymorphisms in XRCC1 gene and treatment outcomes of patients with advanced gastric cancer: a systematic review and meta-analysis. PLoS One. 2014; 9:e85357.
https://doi.org/10.1371/journal.pone.0085357
PMID:24465544

53. Cui Z, Yin Z, Li X, Wu W, Guan P, Zhou B. Association between polymorphisms in XRCC1 gene and clinical outcomes of patients with lung cancer: a meta-analysis. BMC Cancer. 2012; 12:71.
https://doi.org/10.1186/1471-2407-12-71
PMID:22339849

54. Hu Z, Ma H, Chen F, Wei Q, Shen H. XRCC1 polymorphisms and cancer risk: a meta-analysis of 38 case-control studies. Cancer Epidemiol Biomarkers Prev. 2005; 14:1810–8.
https://doi.org/10.1158/1055-9965.EPI-04-0793
PMID:16030121

55. Liu SY, Xue W. XRCC1 Arg194Trp polymorphism and thyroid cancer. J Endocrinol Invest. 2020; 43:749–53.
https://doi.org/10.1007/s40618-019-01155-x
PMID:31820401

56. Yang Z, Liu Z. Potential Functional Variants in DNA Repair Genes Are Associated with Efficacy and Toxicity of Radiotherapy in Patients with Non-Small-Cell Lung Cancer. J Oncol. 2020; 2020:3132786.
https://doi.org/10.1155/2020/3132786
PMID:32684929

57. Formica V, Benassi M, Del Vecchio Blanco G, Doldo E, Martano L, Portarena I, Nardecchia A, Lucchetti J, Morelli C, Giudice E, Rossi P, Anselmo A, Sileri P, et al. Hemoglobin level and XRCC1 polymorphisms to select patients with locally advanced rectal cancer candidate for neoadjuvant chemoradiotherapy with concurrent capecitabine and a platinum salt. Med Oncol. 2018; 35:83.
https://doi.org/10.1007/s12032-018-1141-4
PMID:29721745

58. Pratesi N, Mangoni M, Mancini I, Paiar F, Simi L, Livi L, Cassani S, Buglione M, Grisanti S, Almici C, Polli C, Saieva C, Magrini SM, et al. Association between single nucleotide polymorphisms in the XRCC1 and RAD51 genes and clinical radiosensitivity in head and neck cancer. Radiother Oncol. 2011; 99:356–61.
https://doi.org/10.1016/j.radonc.2011.05.062
PMID:21704413

59. Tengström M, Mannermaa A, Kosma VM, Hirvonen A, Kataja V. XRCC1 rs25487 polymorphism predicts the survival of patients after postoperative radiotherapy and adjuvant chemotherapy for breast cancer. Anticancer Res. 2014; 34:3031–7.
PMID:24922669

60. Li DJ, Xiao D. Association between the XRCC1 polymorphisms and clinical outcomes of advanced NSCLC treated with platinum-based chemotherapy: a meta-analysis based on the PRISMA statement. BMC Cancer. 2017; 17:501.
https://doi.org/10.1186/s12885-017-3487-y
PMID:28743242

61. Liu R, Zhao X, Liu X, Chen Z, Qiu L, Geng R, Guo W, He G, Yin J, Li J, Zhu X. Influences of ERCC1, ERCC2, XRCC1, GSTP1, GSTT1, and MTHFR polymorphisms on clinical outcomes in gastric cancer patients treated with EOF chemotherapy. Tumour Biol. 2016; 37:1753–62.
https://doi.org/10.1007/s13277-015-3935-8
PMID:26314858

62. Liu YP, Ling Y, Qi QF, Zhang YP, Zhang CS, Zhu CT, Wang MH, Pan YD. Genetic polymorphisms of ERCC1-118, XRCC1-399 and GSTP1-105 are associated with the clinical outcome of gastric cancer patients receiving oxaliplatin-based adjuvant chemotherapy. Mol Med Rep. 2013; 7:1904–11.
https://doi.org/10.3892/mmr.2013.1435
PMID:23604281

63. Bartoli M, Jagdale P, Tagliaferro A. A Short Review on Biomedical Applications of Nanostructured Bismuth Oxide and Related Nanomaterials. Materials (Basel). 2020; 13:5234.
https://doi.org/10.3390/ma13225234
PMID:33228140

64. Bermúdez-Guzmán L, Blanco-Saborío A, Ramírez-Zamora J, Lovo E. The Time for Chronotherapy in Radiation Oncology. Front Oncol. 2021; 11:687672.
https://doi.org/10.3389/fonc.2021.687672
PMID:34046365

65. Huang RX, Zhou PK. DNA damage response signaling pathways and targets for radiotherapy sensitization in cancer. Signal Transduct Target Ther. 2020; 5:60.
https://doi.org/10.1038/s41392-020-0150-x
PMID:32355263

66. Lin J, Song T, Li C, Mao W. GSK-3β in DNA repair, apoptosis, and resistance of chemotherapy, radiotherapy of cancer. Biochim Biophys Acta Mol Cell Res. 2020; 1867:118659.
https://doi.org/10.1016/j.bbamcr.2020.118659
PMID:31978503

67. Salles B, Calsou P, Frit P, Muller C. The DNA repair complex DNA-PK, a pharmacological target in cancer chemotherapy and radiotherapy. Pathol Biol (Paris). 2006; 54:185–93.
https://doi.org/10.1016/j.patbio.2006.01.012
PMID:16563661

68. Caldecott KW. XRCC1 and DNA strand break repair. DNA Repair (Amst). 2003; 2:955–69.
https://doi.org/10.1016/s1568-7864(03)00118-6
PMID:12967653

69. London RE. The structural basis of XRCC1-mediated DNA repair. DNA Repair (Amst). 2015; 30:90–103.
https://doi.org/10.1016/j.dnarep.2015.02.005
PMID:25795425

70. Kala R, Shah HN, Martin SL, Tollefsbol TO. Epigenetic-based combinatorial resveratrol and pterostilbene alters DNA damage response by affecting SIRT1 and DNMT enzyme expression, including SIRT1-dependent γ-H2AX and telomerase regulation in triple-negative breast cancer. BMC Cancer. 2015; 15:672.
https://doi.org/10.1186/s12885-015-1693-z
PMID:26459286

71. Saldanha SN, Kala R, Tollefsbol TO. Molecular mechanisms for inhibition of colon cancer cells by combined epigenetic-modulating epigallocatechin gallate and sodium butyrate. Exp Cell Res. 2014; 324:40–53.
https://doi.org/10.1016/j.yexcr.2014.01.024
PMID:24518414

72. Ström CE, Mortusewicz O, Finch D, Parsons JL, Lagerqvist A, Johansson F, Schultz N, Erixon K, Dianov GL, Helleday T. CK2 phosphorylation of XRCC1 facilitates dissociation from DNA and single-strand break formation during base excision repair. DNA Repair (Amst). 2011; 10:961–9.
https://doi.org/10.1016/j.dnarep.2011.07.004
PMID:21840775

73. Mettu RR, Charles T, Landry SJ. CD4+ T-cell epitope prediction using antigen processing constraints. J Immunol Methods. 2016; 432:72–81.
https://doi.org/10.1016/j.jim.2016.02.013
PMID:26891811

74. Zhao E, Zhou C, Chen S. A signature of 14 immune-related gene pairs predicts overall survival in gastric cancer. Clin Transl Oncol. 2021; 23:265–74.
https://doi.org/10.1007/s12094-020-02414-7
PMID:32519178

75. Zhang C, Li Z, Qi F, Hu X, Luo J. Exploration of the relationships between tumor mutation burden with immune infiltrates in clear cell renal cell carcinoma. Ann Transl Med. 2019; 7:648.
https://doi.org/10.21037/atm.2019.10.84
PMID:31930049

76. Yuan B, Li F, Li Y, Chen Y. Construction of a 13-Gene Signature as a Novel Prognostic Marker for Patients with Clear Cell Renal Cell Carcinoma and the Role of XCR1 in Cell Proliferation. Cancer Manag Res. 2020; 12:4017–27.
https://doi.org/10.2147/CMAR.S250126
PMID:33116819

77. Page A, Hubert J, Fusil F, Cosset FL. Exploiting B Cell Transfer for Cancer Therapy: Engineered B Cells to Eradicate Tumors. Int J Mol Sci. 2021; 22:9991.
https://doi.org/10.3390/ijms22189991
PMID:34576154

78. Wennhold K, Shimabukuro-Vornhagen A, von Bergwelt-Baildon M. B Cell-Based Cancer Immunotherapy. Transfus Med Hemother. 2019; 46:36–46.
https://doi.org/10.1159/000496166
PMID:31244580

79. Wennhold K, Weber TM, Klein-Gonzalez N, Thelen M, Garcia-Marquez M, Chakupurakal G, Fiedler A, Schlösser HA, Fischer R, Theurich S, Shimabukuro-Vornhagen A, von Bergwelt-Baildon M. CD40-activated B cells induce anti-tumor immunity *in vivo*. Oncotarget. 2017; 8:27740–53.
https://doi.org/10.18632/oncotarget.7720
PMID:26934557

80. Kim SS, Shen S, Miyauchi S, Sanders PD, Franiak-Pietryga I, Mell L, Gutkind JS, Cohen EEW, Califano JA, Sharabi AB. B Cells Improve Overall Survival in HPV-Associated Squamous Cell Carcinomas and Are Activated by Radiation and PD-1 Blockade. Clin Cancer Res. 2020; 26:3345–59.
https://doi.org/10.1158/1078-0432.CCR-19-3211
PMID:32193227

81. Pardoll DM. The blockade of immune checkpoints in cancer immunotherapy. Nat Rev Cancer. 2012; 12:252–64.
https://doi.org/10.1038/nrc3239
PMID:22437870

82. Merino DM, McShane LM, Fabrizio D, Funari V, Chen SJ, White JR, Wenz P, Baden J, Barrett JC, Chaudhary R, Chen L, Chen WS, Cheng JH, et al, and TMB Harmonization Consortium. Establishing guidelines to harmonize tumor mutational burden (TMB): *in silico* assessment of variation in TMB quantification across diagnostic platforms: phase I of the Friends of Cancer Research TMB Harmonization Project. J Immunother Cancer. 2020; 8:e000147.
https://doi.org/10.1136/jitc-2019-000147
PMID:32217756

83. Kim JY, Kronbichler A, Eisenhut M, Hong SH, van der Vliet HJ, Kang J, Shin JI, Gamerith G. Tumor Mutational Burden and Efficacy of Immune Checkpoint Inhibitors: A Systematic Review and Meta-Analysis. Cancers (Basel). 2019; 11:1798.
https://doi.org/10.3390/cancers11111798
PMID:31731749

84. Louis DN, Ohgaki H, Wiestler OD, Cavenee WK, Burger PC, Jouvet A, Scheithauer BW, Kleihues P. The 2007 WHO classification of tumours of the central nervous system. Acta Neuropathol. 2007; 114:97–109.
https://doi.org/10.1007/s00401-007-0243-4
PMID:17618441
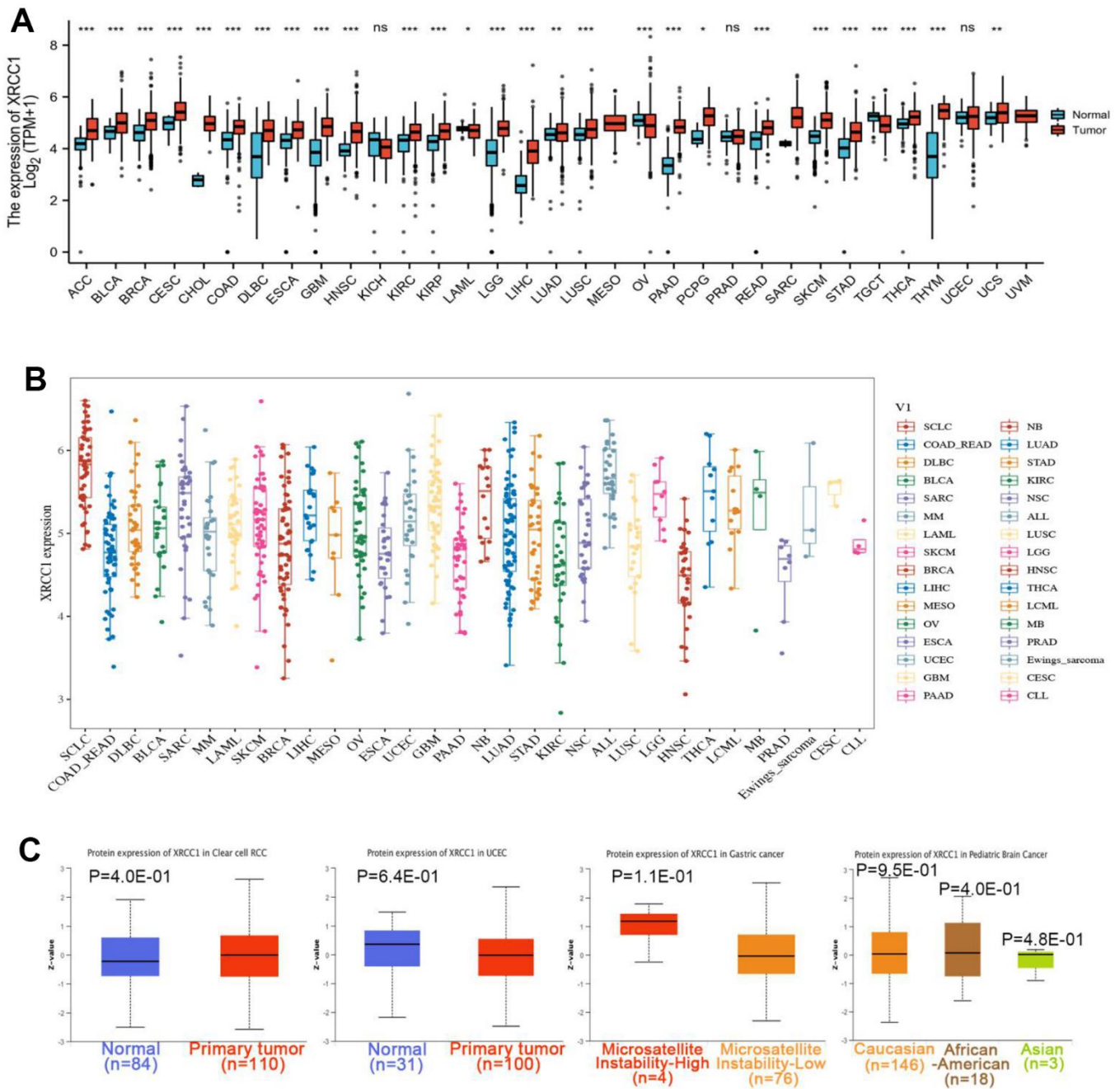
**Supplementary Figure 1.** Wilcoxon rank sum test was performed to explore the differential expression of XRCC1 between normal and tumor tissues in combination with TCGA and GTEx dataset (**A**). We analyzed the cell line expression matrix of 32 tumors from TCGA database (**B**). The protein expression of XRCC1 genes that were not significantly different was presented (**C**). (ns, P≥0.05; *, P< 0.05; **, P<0.01; ***, P<0.001).
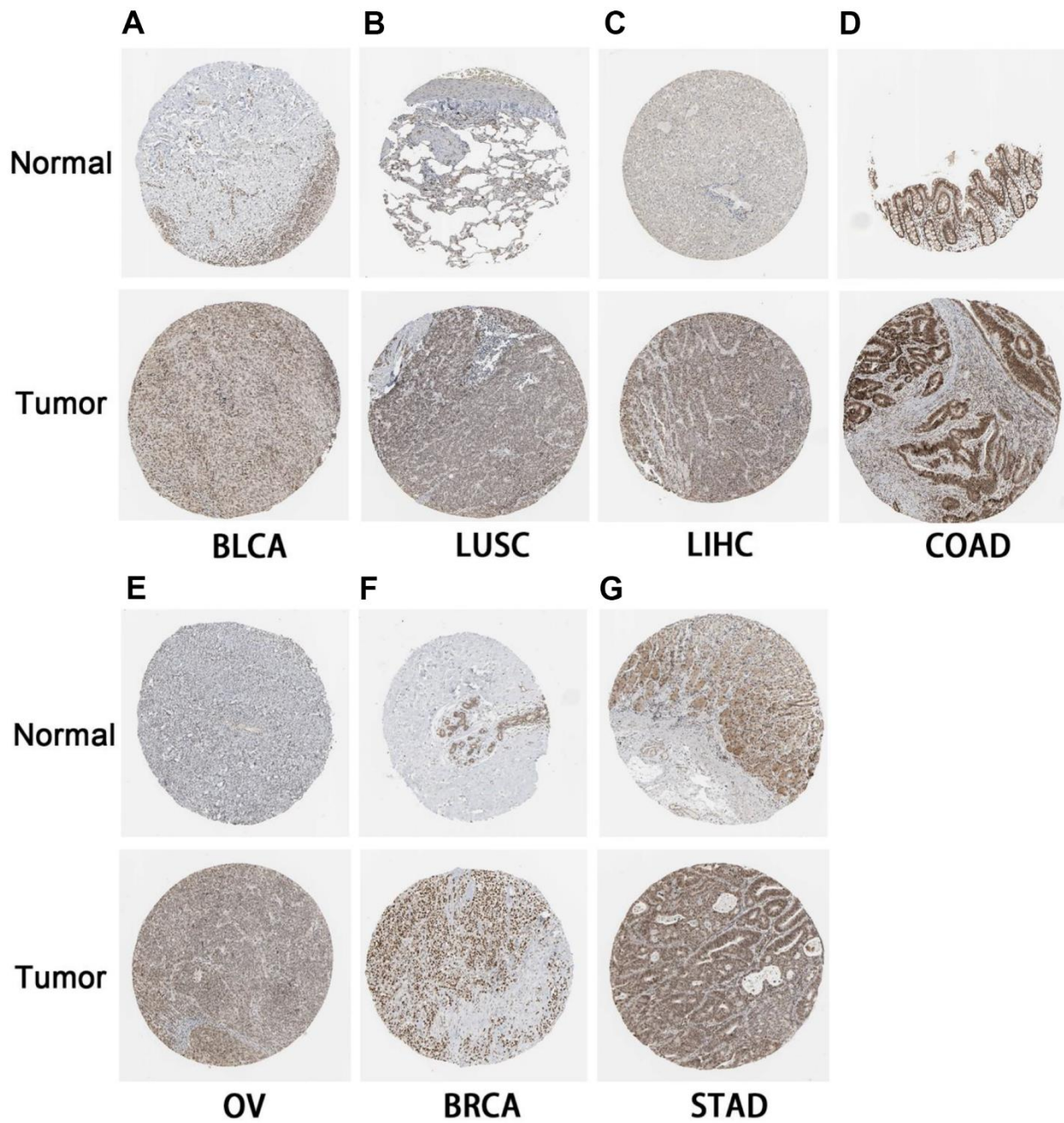
Supplementary Figure 2. HPA database verifies the expression of XRCC1 gene in seven tumors. The expression of XRCC1 gene in BLCA (**A**), LUSC (**B**), LIHC (**C**), COAD (**D**), OV (**E**), BRCA (**F**), and STAD (**G**) is significantly higher than that in the corresponding normal tissues.
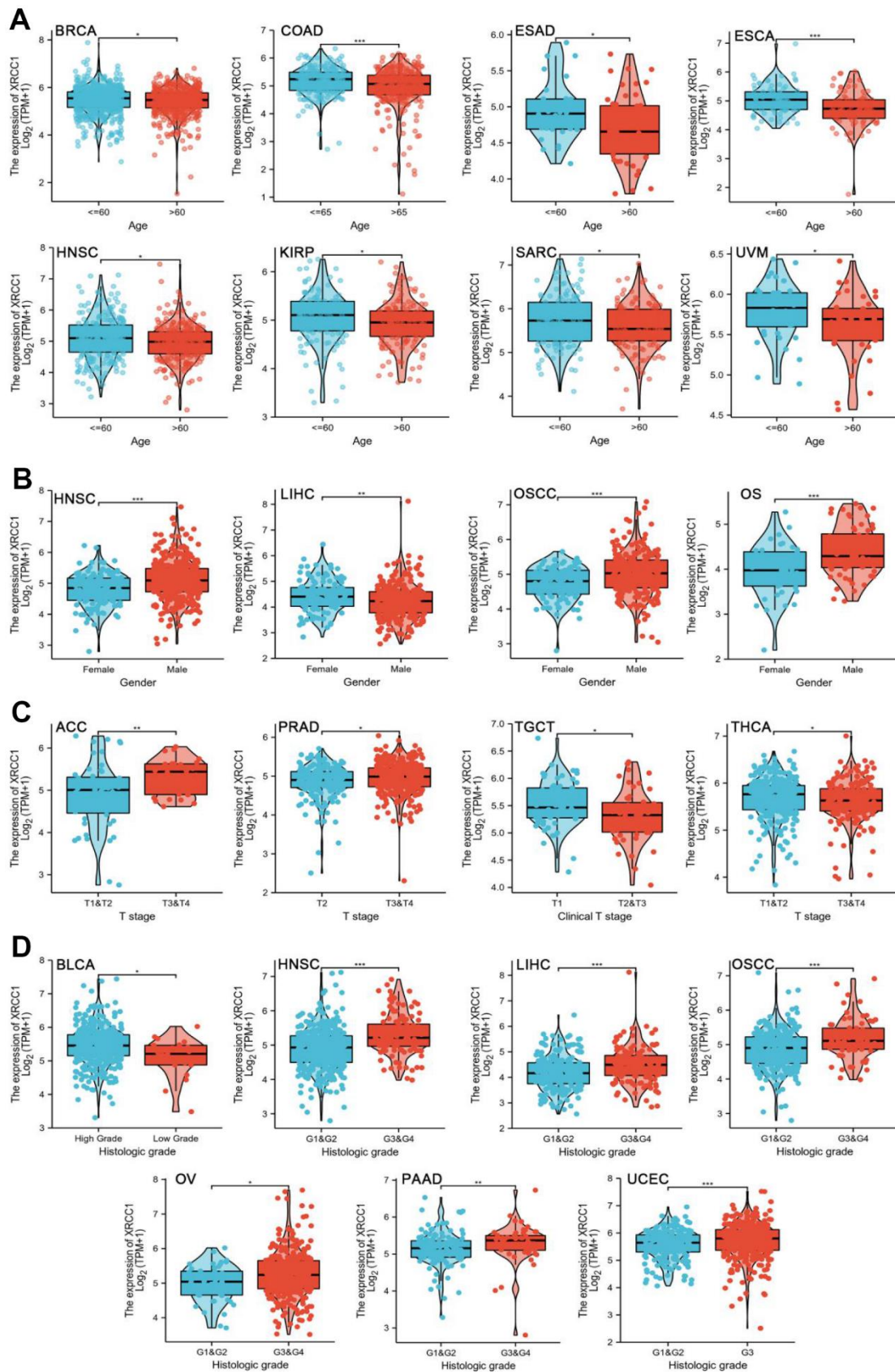
Supplementary Figure 3. Association between XRCC1 gene expression and clinical characteristics, including (**A**) Age, (**B**) Gender, (**C**) T stage, (**D**) Histologic grade.
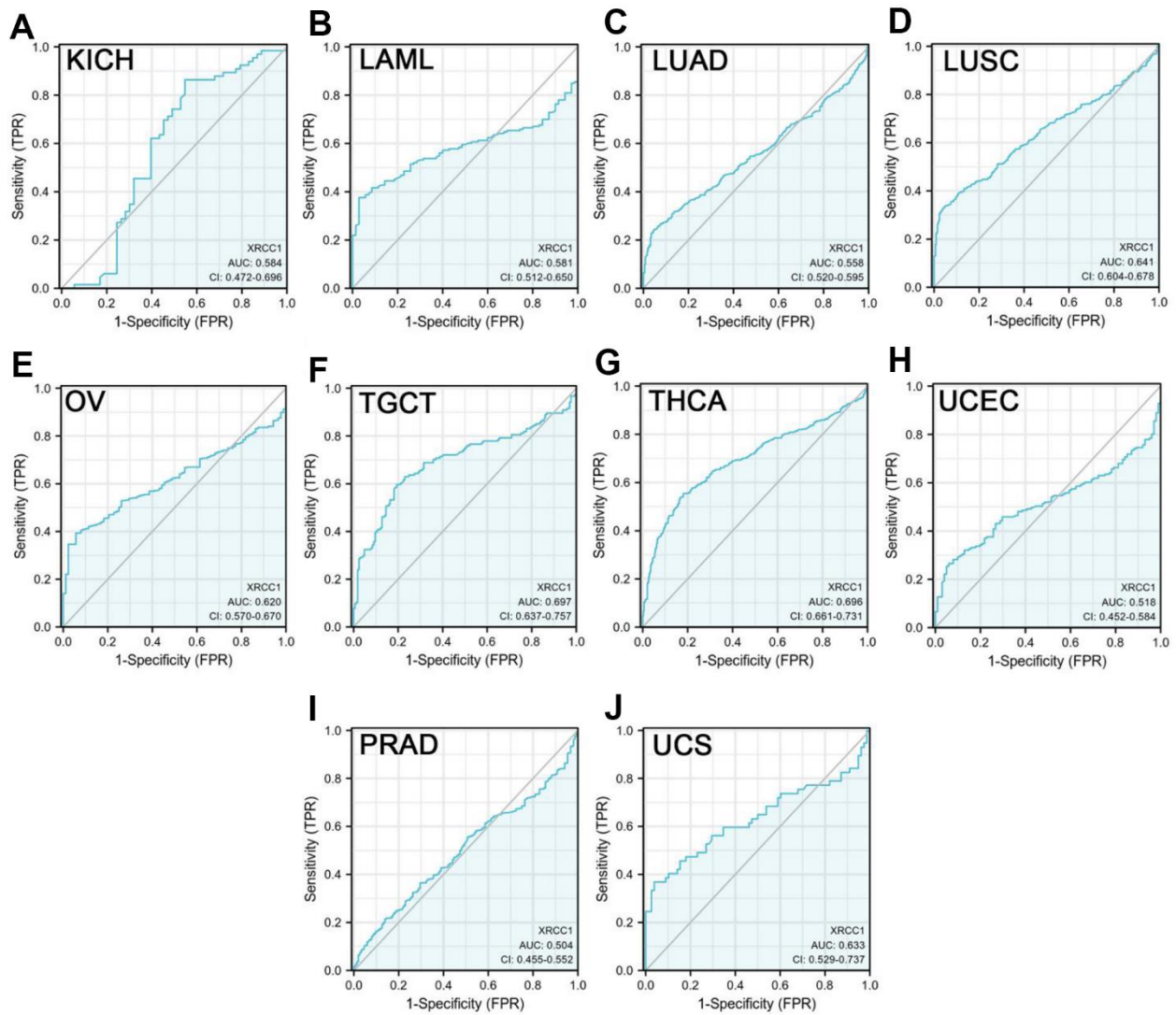
Supplementary Figure 4. ROC curve showed the efficiency of XRCC1 expression level to distinguish tumor tissue from non-tumor tissue. (**A**) KICH, (**B**) LAML, (**C**) LUAD, (**D**) LUSC, (**E**) OV, (**F**) TGCT, (**G**) THCA, (**H**) UCEC, (**I**) PRAD, (**J**) UCS.
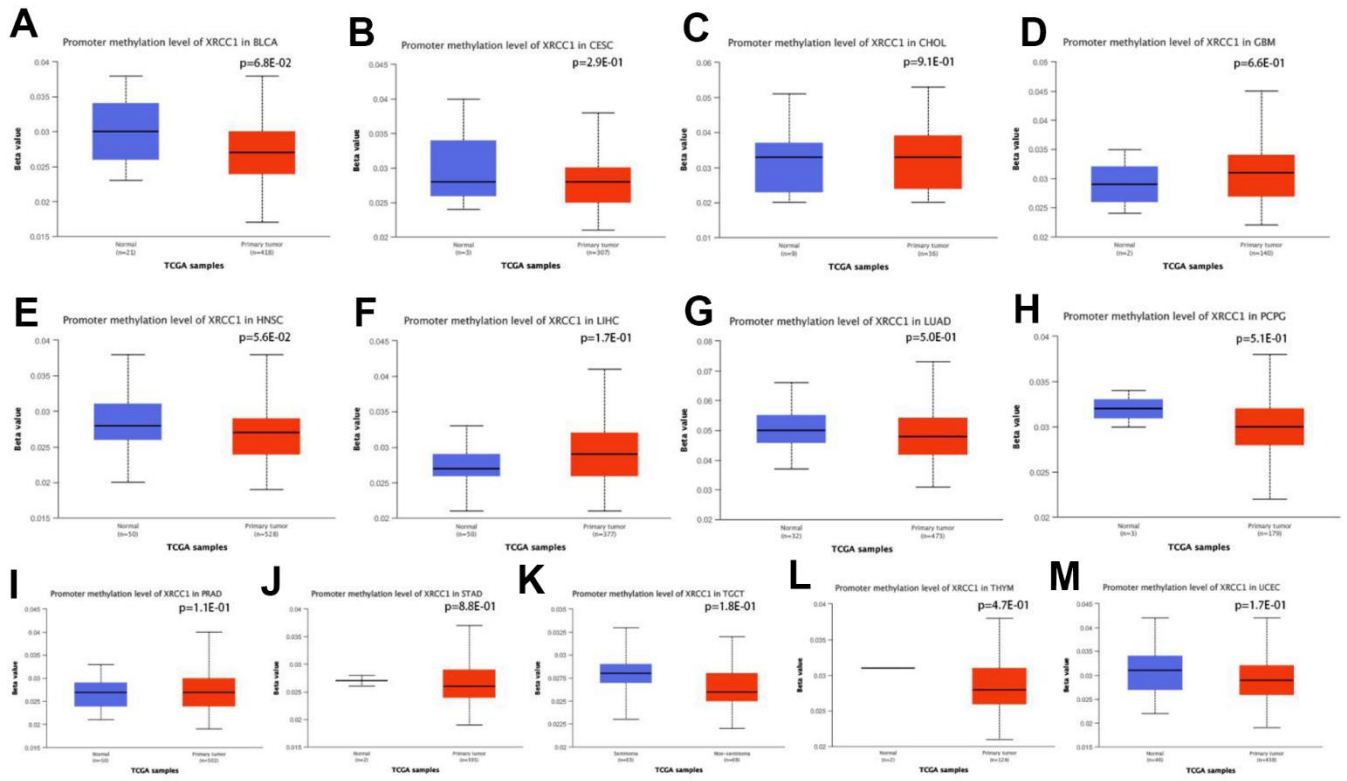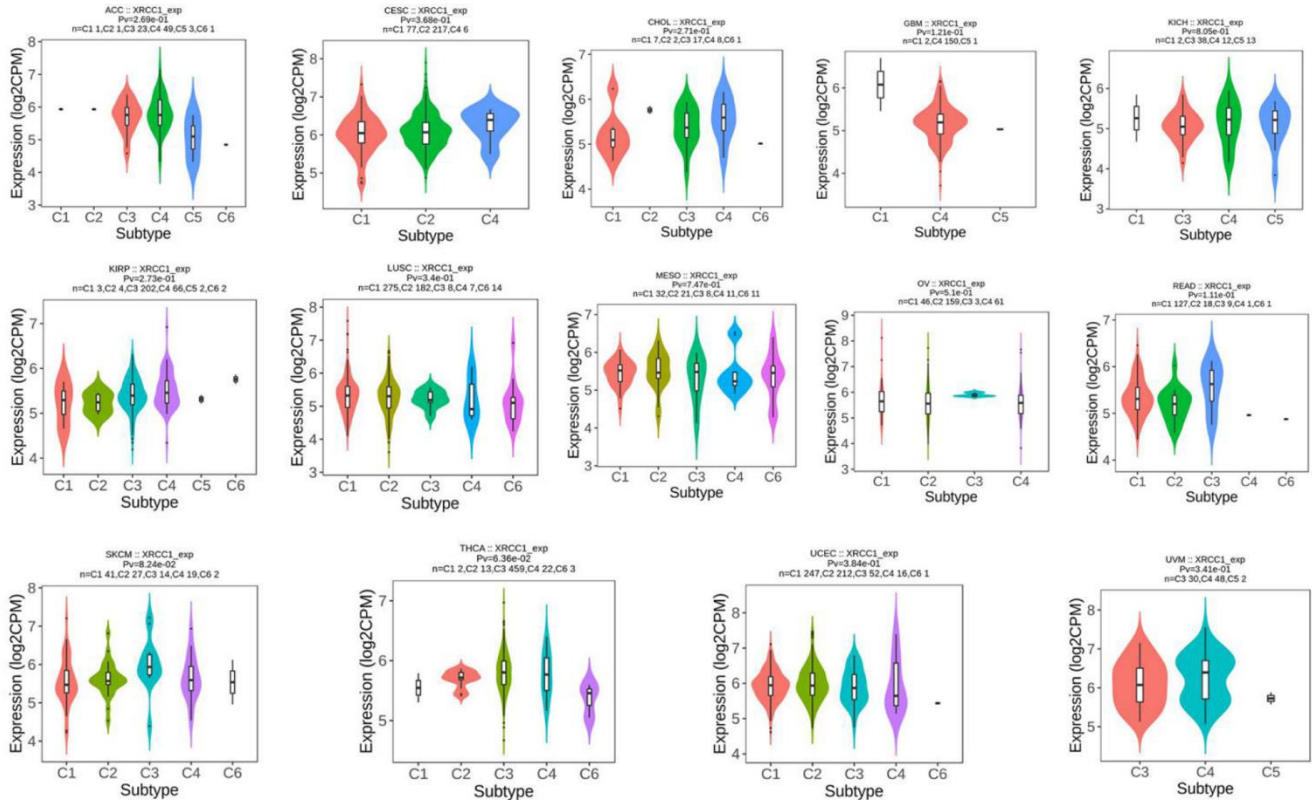
Supplementary Figure 5. Promoter methylation level of XRCC1 in pan-cancer. (**A**) in BLCA, (**B**) in CESC, (**C**) in CHOL, (**D**) in GBM, (**E**) in HNSC, (**F**) in LIHC, (**G**) in LUAD, (**H**) in PCPG, (**I**) in PRAD, (**J**) in STAD, (**K**) TGCT, (**L**) THYM, (**M**) UCEC.
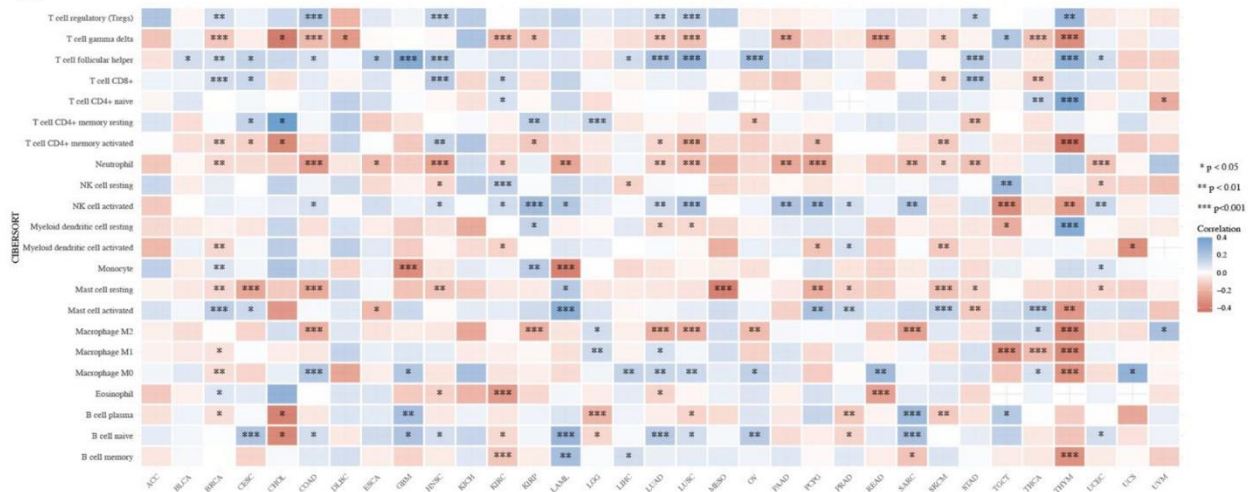
A immune subtype
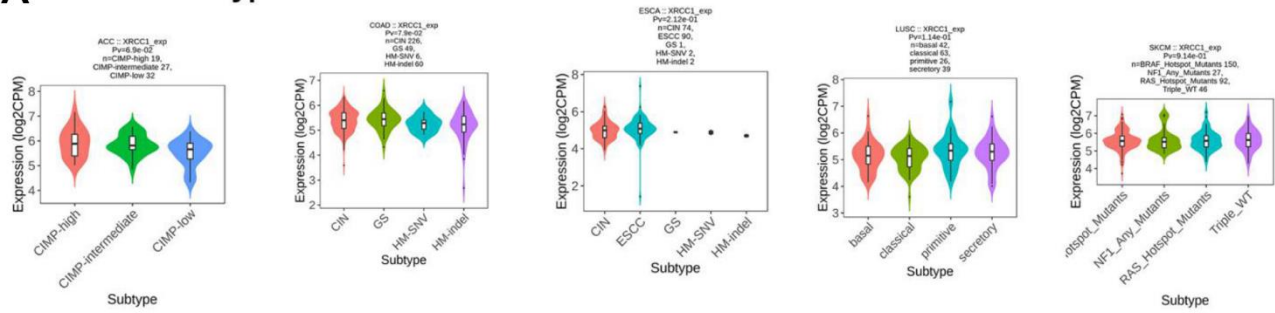
B molecular subtype

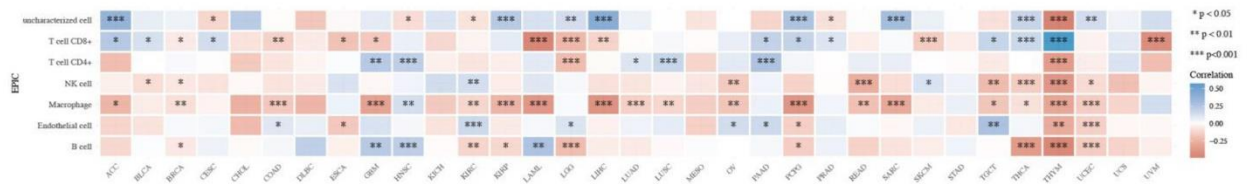**Supplementary Figure 6.** The relationship between XRCC1 expression and pan-cancer immune subtypes (**A**) and molecular subtypes (**B**).

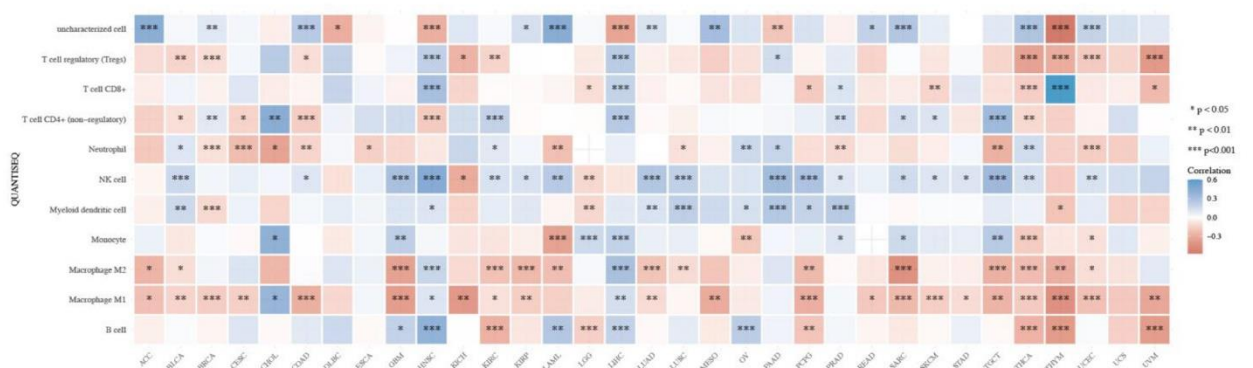**Supplementary Figure 7.** We investigated the correlation of XRCC1 gene expression with the level of infiltration of various immune cells via CIBERSOR (**A**), EPIC (**B**), MCPCOUNTER (**C**), QUANTISEQ (**D**). (P≥0.05; *, P< 0.05; **, P<0.01; ***, P<0.001).

Supplementary Tables

Supplementary Table 1. Results of analyses of GO and KEGG.

Ontology	ID	Description	GeneRatio	BgRatio	P-value	p.adjust	q-value
BP	GO:0000070	mitotic sister chromatid segregation	31/911	151/18670	7.62e-12	1.50e-09	1.29e-09
BP	GO:0140014	mitotic nuclear division	38/911	264/18670	2.13e-09	2.01e-07	1.73e-07
BP	GO:0031577	spindle checkpoint	9/911	34/18670	2.62e-05	7.49e-04	6.47e-04
BP	GO:0071103	DNA conformation change	31/911	327/18670	3.30e-04	0.006	0.005
BP	GO:0007093	mitotic cell cycle checkpoint	19/911	165/18670	4.50e-04	0.008	0.007
CC	GO:1902495	transmembrane transporter complex	63/955	324/19717	1.43e-21	1.74e-19	1.32e-19
CC	GO:0044306	neuron projection terminus	30/955	138/19717	3.00e-12	1.12e-10	8.47e-11
CC	GO:0072686	mitotic spindle	15/955	109/19717	2.43e-04	0.002	0.001
CC	GO:0098687	chromosomal region	32/955	349/19717	4.26e-04	0.003	0.002
CC	GO:0005876	spindle microtubule	10/955	59/19717	4.90e-04	0.003	0.002
MF	GO:0022836	gated channel activity	67/889	343/17697	3.50e-22	1.45e-19	1.22e-19
MF	GO:0030594	neurotransmitter receptor activity	36/889	117/17697	3.24e-19	3.58e-17	3.03e-17
MF	GO:0098960	postsynaptic neurotransmitter receptor activity	18/889	52/17697	2.96e-11	1.35e-09	1.14e-09
MF	GO:0008017	microtubule binding	28/889	246/17697	4.65e-05	7.06e-04	5.98e-04
MF	GO:0035173	histone kinase activity	5/889	17/17697	0.001	0.012	0.010
KEGG	hsa04080	Neuroactive ligand-receptor interaction	65/364	341/8076	1.95e-24	5.19e-22	4.38e-22
KEGG	hsa04727	GABAergic synapse	20/364	89/8076	1.63e-09	8.65e-08	7.29e-08
KEGG	hsa04024	cAMP signaling pathway	29/364	216/8076	1.07e-07	3.56e-06	3.00e-06
KEGG	hsa04110	Cell cycle	16/364	124/8076	1.32e-04	0.002	0.002
KEGG	hsa04014	Ras signaling pathway	21/364	232/8076	0.002	0.017	0.015

Supplementary Table 2. GSEA analysis results.

GSEA-GO

ID	ES	NES
GO_NUCLEAR_CHROMOSOME	0.583	4.832
GO_TRANSCRIPTION_REGULATOR_ACTIVITY	0.586	4.73
GO_REGULATORY_REGION_NUCLEIC_ACID_BINDING	0.558	4.105
GO_POSITIVE_REGULATION_OF_RNA_BIOSYNTHETIC_PROCESS	0.528	4.077
GO_MITOTIC_CELL_CYCLE_CHECKPOINT	0.679	2.983
GO_CELLULAR_RESPONSE_TO_DNA_DAMAGE_STIMULUS	0.541	2.904
GO_REGULATION_OF_NUCLEAR_DIVISION	0.598	2.777
GO_DNA_REPLICATION	0.573	2.619
GO_DNA_INTEGRITY_CHECKPOINT	0.653	2.587
GO_DNA_REPAIR	0.565	2.578
GO_DNA_PACKAGING	0.519	2.475
GO_DNA_BINDING_TRANSCRIPTION_FACTOR_BINDING	0.647	2.433
GO_MITOTIC_DNA_INTEGRITY_CHECKPOINT	0.675	2.379
GO_DNA_BIOSYNTHETIC_PROCESS	0.568	1.924
GO_NEGATIVE_REGULATION_OF_IMMUNE_SYSTEM_PROCESS	0.481	1.906
GO_SIGNAL_TRANSDUCTION_IN_RESPONSE_TO_DNA_DAMAGE	0.549	1.86

GSEA-Reactome

ID	ES	NES	p.adjust
REACTOME_CELL_CYCLE	0.633	4.126	0.006
REACTOME_CELL_CYCLE_MITOTIC	0.632	3.966	0.006
REACTOME_CELL_CYCLE_CHECKPOINTS	0.681	3.769	0.006
REACTOME_M_PHASE	0.587	3.338	0.006
REACTOME_MITOTIC_SPINDLE_CHECKPOINT	0.69	3.22	0.006
REACTOME_MITOTIC_METAPHASE_AND_ANAPHASE	0.626	3.169	0.006
REACTOME_MITOTIC_PROMETAPHASE	0.607	3.127	0.006
REACTOME_SEPARATION_OF_SISTER_CHROMATIDS	0.637	3.101	0.006
REACTOME_DNA_REPAIR	0.658	2.581	0.006
REACTOME_G2_M_CHECKPOINTS	0.676	2.573	0.006
REACTOME_GABA_RECEPTOR_ACTIVATION	-0.484	-1.996	0.012
REACTOME_NEUROTRANSMITTER_RELEASE_CYCLE	-0.58	-2.197	0.007
REACTOME_NEUROTRANSMITTER_RECEPTORS_AND_POSTSYNAPTIC_SIGNAL_TRANSMISSION	-0.394	-2.451	0.007
REACTOME_SIGNALING_BY_GPCR	-0.303	-2.52	0.008
REACTOME_TRANSMISSION_ACROSS_CHEMICAL_SYNAPSES	-0.413	-2.881	0.007
REACTOME_NEURONAL_SYSTEM	-0.414	-3.271	0.008